Master's Thesis

Master's degree in Energy Engineering

Analysis of the potential of solar-based energy technologies to meet the energy demand of a hospital

REPORT

Author: Guillem Guerrero Almirall
Director: Alba Ramos Cabal

Call: September 2020

Escola Tècnica Superior
d'Enginyeria Industrial de Barcelona

Abstract

The objective of this thesis is to design a renewable energy system which supplies electrical and/or thermal energy to Hospital de Sant Pau, in Barcelona. This system is based in solar power harnessing technologies.

With this purpose, the available technologies in the market are studied and the available data is analyzed: temperature, solar irradiation, weather and the hospital's energy demand. Knowing these data, three installation alternatives are proposed, based on photovoltaic, thermal or hybrid solar panels, respectively.

For each option, the number and distribution of panels is calculated and their energy output throughout the year is determined by using the aforementioned weather data. Since this information is available for every hour of a year, the calculations can be carried out with high detail. The energy output is optimized by adjusting the orientation of the panels and the separation between rows of panels.

These energy outputs, emissions savings, costs, payback times and economic revenue of these alternatives have been studied in order to choose the most suitable system amongst them. The three alternatives have proven similar rentability and emissions savings per euro invested and have proven to be viable options. However, the solar thermal option has been chosen due to its slight advantages in economic terms in front of the hybrid option whilst providing an almost equal amount of energy (and thus, of emissions savings). Finally, a Life Cycle Assessment has been carried out for the chosen system.

In conclusion, any of the studied solar-based renewable energy production systems is an economically viable option for the hospital, even if they can only cover a small percentage of the building's vast energy demand. Environmentally speaking, it can be assured that at least the solar thermal project, which has been analyzed more deeply, is also viable, implying an important reduction of greenhouse gases emissions.

Index

INDEX 4

1. INTRODUCTION 7

1.1. Context 7

1.1.1. Normative 9

1.2. Justification 10

1.3. Objectives 10

1.4. Scope 11

2. SITE IDENTIFICATION 12

2.1. Site description 12

2.2. Location 13

2.3. Climate 14

2.4. Solar resource 16

3. AVAILABLE TECHNOLOGIES 18

3.1. Solar photovoltaic panels 18

3.1.1. Photoelectric effect 18

3.1.2. P-N junction 18

3.1.3. The photovoltaic cell 18

3.1.4. Structure of a PV panel 19

3.1.5. Types of photovoltaic panels 20

3.1.6. Arrange of solar panels 21

3.1.7. Connectivity and electric components 22

3.1.8. Operation 23

3.1.9. Efficiency 23

3.1.10. Shade mismatch 24

3.2. Solar thermal 24

3.2.1. How it works 24

3.2.2. Parts 25

3.2.3. Flat plates 25

3.2.4. Low-temperature 25

3.2.5. Medium-temperature 26

3.2.6. Efficiency 27

3.3. Solar thermo-electric 27

3.3.1. Parabolic Trough Collectors 27

3.3.2. Efficiency 28

3.4. Solar hybrid 28

3.4.1. Structure of the PVT panel 29
3.4.2. Arrange 30
3.4.3. Types 30
3.4.4. Operation and efficiency 30
3.5. Connection systems 30
3.6. Storage systems 31
3.6.1. Electrical batteries 31
3.6.2. Thermal storage 33

4. LOAD DESCRIPTION 35
4.1. Electrical load 35
4.2. Thermal load 39

5. INSTALLATION SIZING AND DESIGN 41
5.1. Available area 41
5.2. Photovoltaic modules 43
5.3. Solar thermal modules 50
5.4. Hybrid photovoltaic/thermal modules 51

6. ECONOMIC ANALYSIS 53
6.1. Photovoltaic panels 53
6.2. Thermal panels 54
6.3. Hybrid PVT panels 56
6.4. Comparison 58

7. ENVIRONMENTAL ANALYSIS 60
7.1. Emissions 60
7.2. Life Cycle Assessment 60

CONCLUSIONS 65

ACKNOWLEDGEMENTS 67

BIBLIOGRAPHY 68

1. Introduction

1.1. Context

At the present time, one of the major concerns worldwide is climate change caused by global warming, and how to stop this temperature raise by eradicating, or at least mitigating, the greenhouse gases (GHG) emissions. Several countries have set as one of their main objectives the reduction of these gases on the short- and mid- term and the achievement of net-zero emissions on the long term.

In Spain, the installed power from renewable sources surpassed that of non-renewable sources in 2019, reaching a 50.1% of the total installed power in the country. This increment has been due mainly to the 89.2% increase in solar photovoltaic systems, which represent now an 8.1% of the installed power in the country. Solar thermal energy accounts for another 2.1% of the installed power, whilst the main renewable energy source in the country is wind power, representing a 23.4% of Spanish installed power [1].

Around a 38.9% of the 264,635 GWh of electrical energy generated in Spain in 2019 was obtained from renewable sources, according to *Red Eléctrica Española*. This percentage is slightly lower than that of 2018, since the hydraulic power plants generated a 28% less due to the low amount of precipitations. However, the rest of available renewable technologies increased their production in a 10.5% in average in 2019 [1]. The electricity generation in Spain in 2018 and 2019 is shown in Figure 1, per source and in percentage over the total.

	2018	2019
PUMPED STORAGE	0.8	0.7
NUCLEAR	21.5	22.6
COAL	14.1	4.3
COMBINED CYCLE	10.7	20.7
COGENERATION	11.7	12.0
NON-RENEWABLE WASTE	0.9	0.8
RENEWABLE WASTE	0.3	0.3
WIND	19.8	21.5
HYDRO	13.8	10.0
SOLAR PHOTOVOLTAICS	3.0	3.6
SOLAR THERMAL	1.8	2.1
OTHER RENEWABLES	1.4	1.5

	2018	2019
RENEWABLES	40.2	38.9
NON-RENEWABLES	59.8	61.1

Figure 1 - Electricity generation by source in Spain in 2018 and 2019 [1].

Another important improvement in Spanish electrical system is the substitution of an important part of coal- and fuel-powered generation (66% and 15% respectively) by combined cycle natural gas-fueled power plants. This technology is not renewable and accounts for more than

a 40% of the greenhouse gases emissions of the electrical system, but its higher efficiency and far lower emission factor than that of coal- or fuel-powered power plants allows for a significant reduction of emissions [1].

Altogether, the emissions derived from the production of energy from coal, fuel and gas accounted for around 36.1 million tonnes of CO_2-equivalent in 2018, and 36.9 in 2019. This increase is almost negligible compared to the fact that these emissions were produced in the generation of a 28% more energy than in 2018 with these three technologies [1] [2].

In global, and partly due to this gasification, the emissions of the Spanish electrical system in 2019 were around 50 million tonnes of CO_2-equivalent, a 23% less than on the previous year and the lowest since record is kept (1990) [1]. The emissions per unit of energy generated have also decreased to 0.19 tonnes of CO_2-equivalent per MWh_e generated [2]. The evolution of these emissions in the last decade may be observed in Figure 2.

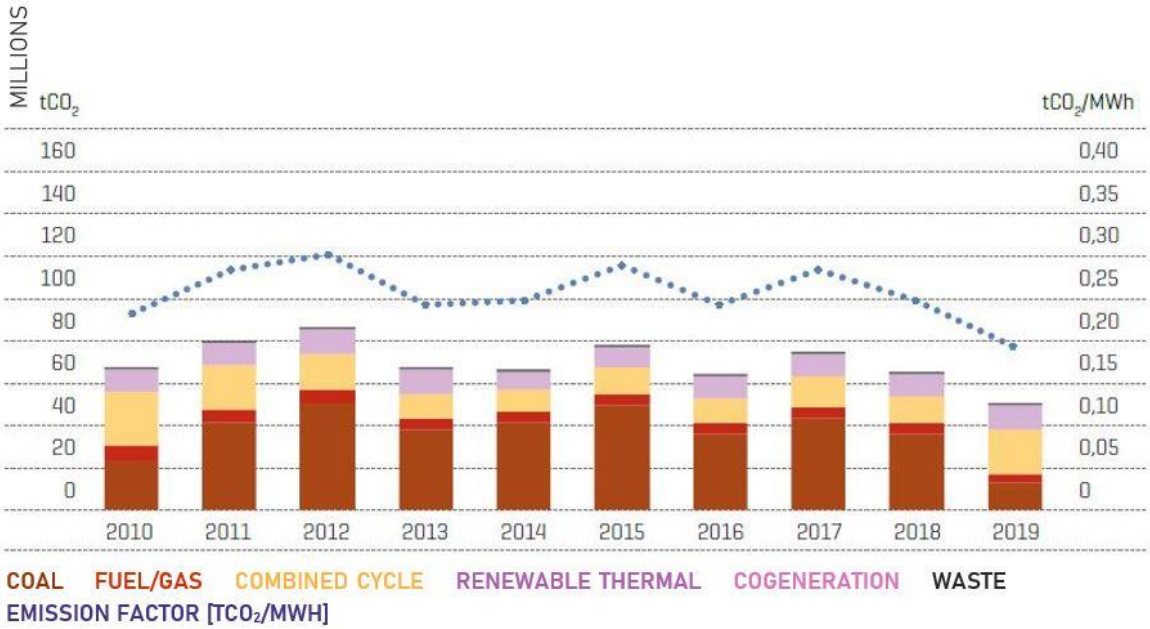

Figure 2 - CO_2-equivalent emissions in Spanish electrical system (2010 - 2019) [1].

The European Union has also established mid- and long-term plans in order to reduce the member states' greenhouse gases emissions. One of the most relevant of these objectives is manifested in the European Emission Standards, presented in several consecutive emission limits for new-made vehicles in the EU, each one lower than the previous one. Nowadays, the Euro 6d normative is applied [3].

Another crucial objective is the 2030 strategy, decreed in 2018. This legislation aims for a reduction of 40% on greenhouse gas emissions related to 1990 levels, a production of 32% of

the EU energy from renewable sources and a 32.5% improvement in energy efficiency [4]. This strategy is on the line of the EU's objective to accomplish a net-zero emission level for the year 2050 [5].

1.1.1. Normative

There are several normatives and legislations which apply regarding the installation and harnessing of renewable energy. Since Spain is a part of the European Union, both Spanish and European legislation may apply.

Regarding Spanish normative, the *Real Decreto 244/2019*, of 5 April, establishes two modalities of electricity self-consumption: with and without surplus. Producers with surplus may sell this surplus to the distribution grid, whilst those without surplus may not, even if they had. Producers with surplus whose installed power does not exceed 100 kW and comes from renewable sources may be paid by the distributor for the energy surplus that is injected to the grid. Installations of less than 15 kW on urbanized soil won't require any access or connection permits [6].

This Decree amends the previous 24/2013 Law, of 26 December, which established that if there was any exchange of energy with the grid, there will be a charge on the concept of the usage of the distribution grid. This law also entrusts the state and regional administrations to improve the efficiency of energy generation, transformation and consumption systems in industrial, business and residential buildings [7].

The Basic Document HE (of energy savings, in Spanish) establishes the ground for the limitation of energy consumption in thermal and lighting installations. It also sets that the energy demand of domestic hot water and pool heating must be covered in at least a 70% by renewable or cogeneration sources and settles that all new big buildings or reformations must include a renewable energy generation system [8].

Concerning European normative, the Directive 2010/31/UE establishes that all new public buildings since 2019 must be nearly zero-energy buildings (NZEB), and at the latest at the end on 2020 all new buildings must also be NZEB. It also lays the foundations for HVAC system inspections and for energy efficiency certificates [9].

The directive 2012/27/UE settles the objective of saving around a 20% of the primary energy consumption in the European Union and establishes that all countries must reform a 3% of the central administration every year. It also promotes energy efficiency in heating and refrigeration systems [10].

The European Union Directive 2018/2001 encourages member states to provide incentives for the maximum integration of renewable energy in the electric market and establishes the target

for the share of energy from renewable sources for each country in the EU. Furthermore, it states that in 2030 at least a 32% of the gross energy consumption in the EU must come from renewable energies, though a revision in 2023 could imply an increase on this percentage. In the transport sector, the share of energy coming from renewable sources should be at least a 14% by 2030 [11].

It also establishes the rules which need to be applied when calculating the greenhouse gas impact of fossil fuels and biofuels and sets typical values for the emission of carbon dioxide for cultivation, processing or transport for different biomass fuels [11]. This Directive amends the previous Directive 2009/28/EC on the promotion of the use of energy from renewable energies, which presented analogous objectives, though with a smaller percentage of renewable energy as the objective, and with the scope on the year 2020 [12].

1.2. Justification

Hospitals are some of the buildings with the highest energy consumption per surface unit, due to the fact that they work 24 hours a day and are equipped with high energy consumption equipment such as defibrillators, respirators, surgical units, amongst other machinery and equipment. In the European Union, the average yearly energy consumption for buildings is 180 kWh/m^2, and in Spain this number is slightly lower since it is located in the Mediterranean area's temperate climate [13].

A renewable-based energy generation system in a hospital would not only lower the hospital's energy consumption and CO_2 emissions, but also those produced by the city of Barcelona. Like in most cities, due to the high population density and low free space, most of the energy consumed in this city is produced elsewhere. In fact, only 139 GWh of the 14,995 GWh yearly consumption were produced in Barcelona (2017 data obtained from [14]).

Consequently, this installation would not only reduce the energy dependence of the hospital and the city, it would also ease the electricity transmission load inside Barcelona and in its surroundings.

1.3. Objectives

The main objective of this project is to design a self-consumption energy system which allows the hospital to reduce its energetic dependency on the grid. Indirectly, this decrease on energy dependency will also affect the city of Barcelona, being one of the areas with one of the higher energy consumption and lower production in Spain.

Provided the capital importance of economy in all projects, the designed installation must be profitable, even if it is on the medium or long term. It is crucial that the amount of the revenue at the end of the project exceeds the initial investment.

The designed system will be based on renewable sources, specifically on any way of harnessing solar power. Obtaining clean energy will imply a decrease of the greenhouse gases emissions of the hospital and consequently the carbon footprint of Barcelona will also be reduced, whilst promoting renewable energy sources.

Finally, an environmental analysis of the project will be carried out, evaluating the greenhouse gases emissions saved by the designed installation both in terms of energy generation and in terms of the construction of the elements that are required for the system.

1.4. Scope

This project will be based on the available data and will be as precise as this data allows. In some other cases, reasonable suppositions may be made when in lack of data. In any case, the scope of the project will be only theoretical: though calculations will be carried out as accurately as possible, the installation will remain on paper.

The solar resource at the site of the hospital will be analyzed in order to estimate the energy extraction potential. The currently available technologies, including solar photovoltaic, thermal and hybrid panels, as well as storage systems, will be studied. This way, the available technology alternatives and their advantages and disadvantages will be known in order to choose the most adequate one.

The hospital's consumption data will be taken as precise as it is available, though when exact data are not obtainable, realist data will be extrapolated from other hospitals' data so as to obtain feasible and realistic consumption curves.

In both energy consumption data and meteorological data, the studied time interval is a natural year, which is considered as a large enough time lapse as to carry out the calculations. Though the way in which both meteorological data and energy consumption vary every year is impossible to predict with exactitude, the results obtained from the data of a whole year are considered to be accurate enough.

In all the project, real or exact data will be used when possible, and when it is not possible, they will be reasonably estimated and used for the calculations.

2. Site identification

2.1. Site description

The chosen building for this study is Hospital de la Santa Creu i Sant Pau, in Barcelona. At this site, in 1401, the six existing hospitals of the city were unified into one, the Hospital de la Santa Creu. Five hundred years later, thanks to a generous donation of the banker Pau Gil, the hospital could be rebuilt in order to answer the medical needs of the ever-growing city. The name of the hospital was then adapted to honor the donor's will.

This new building, inaugurated in 1930, was of Modernist style, designed by the architect Lluís Domènech i Montaner. It was declared World Heritage by UNESCO in 1997 due to the building being a "masterpiece of the imaginative and exuberant Art Nouveau" [15]. In 2009, a new hospital was built in the northern edge of the hospital's terrain, leaving the Modernist part as administration and visiting area and transferring the medical activities to the new buildings.

This hospital consists mainly in two parts: The Modernist area, with decorated, two-story separate buildings amidst gardens, and the new hospital area, which consists of five higher blocks, each one dedicated to different medical activities. This distribution can easily be identified in Figure 3.

Figure 3 - Aerial picture of the hospital area.

Since the modernist area of the hospital is a World Heritage Site, it must be preserved and not modified in any way. Consequently, the study will only consider the new hospital (considering then its buildings, roofs and gardens) as the possible site for the installation.

2.2. Location

As mentioned above, Hospital de la Santa Creu i Sant Pau is located in the Horta-Guinardó district of the city of Barcelona, located in north-eastern Spain, as Figure 4 shows. The geographical coordinates of this hospital are 41° 24′ 50″ North and 2° 10′ 28" East.

Figure 4 - Location of the hospital.

The terrain in which the hospital is built is a roughly 382 x 348 meters, 132,521 m^2 rectangular plot, slightly chamfered at its corners, as shown in Figure 5 below. This terrain is located at between 52 and 85 meters above sea level, in an approximately East-South-East-facing 7% slope. The built area inside this plot accounts for a total of 113,615 m^2.

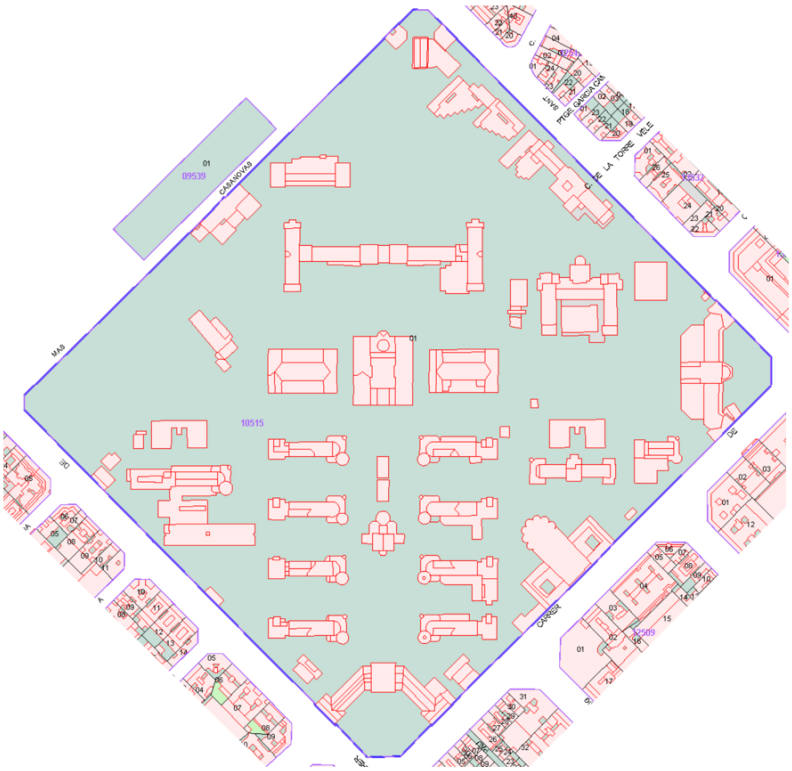

Figure 5 – Plan of the hospital's terrain [16].

2.3. Climate

Barcelona is located around 41º North, on the Mediterranean coast, an area where, according to the Köppen-Geiger climate classification, with a hot-summer Mediterranean climate (Csa) [17]. Csa climate can be found in areas of California, Chile, South Africa, Australia or the Middle East, but it is located mostly at coastal areas around the Mediterranean Sea, as Figure 6 below shows.

Figure 6 – Distribution of hot-summer Mediterranean climate (Csa) around the Mediterranean Sea [18].

In Spain, this climate is extended along the Mediterranean coast, thus including Barcelona, and most of the southwest of the country, as Figure 7 shows:

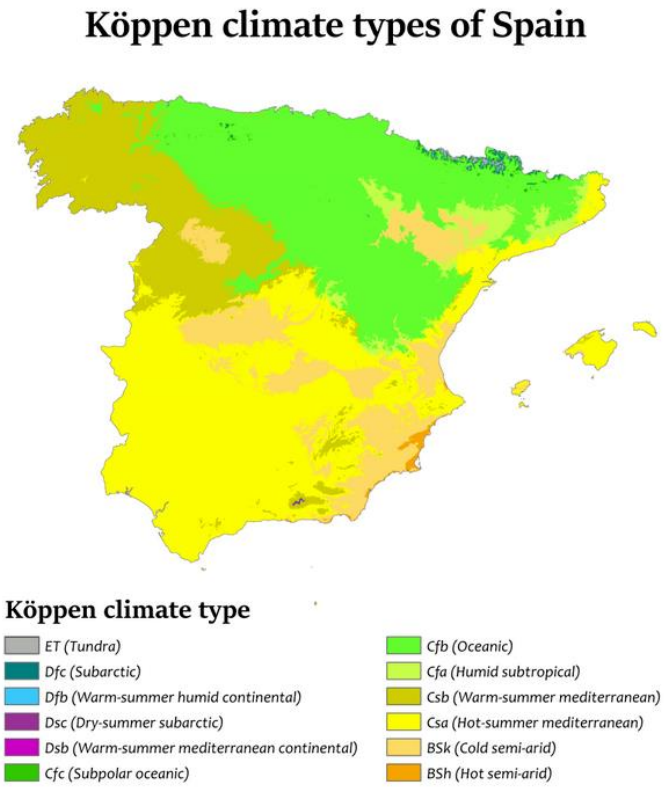

Figure 7 – Distribution of climate zones in Spain [19].

This climate is characterized mainly by presenting hot and dry summers as well as mild and wet winters. It was also called the “olive climate” by Wladimir Köppen [20], since its distribution, especially around the Mediterranean area, is almost identical to the historical distribution of olive trees.

2.4. Solar resource

Barcelona has an abundant solar resource, with an average of 298 days which are at least partly sunny per year [21]. The average annual global horizontal irradiation at this location is, according to the Global Solar Atlas [22], around 1,610 kWh/m^2. From the same source, Figure 8 showing the path of the sun throughout the year, especially considering the possible shade that the nearby environment may cause. Given the fact that the height of the new hospital is similar to that of the buildings nearby, they will not shade the panels as long as they are located in the roof of the hospital.

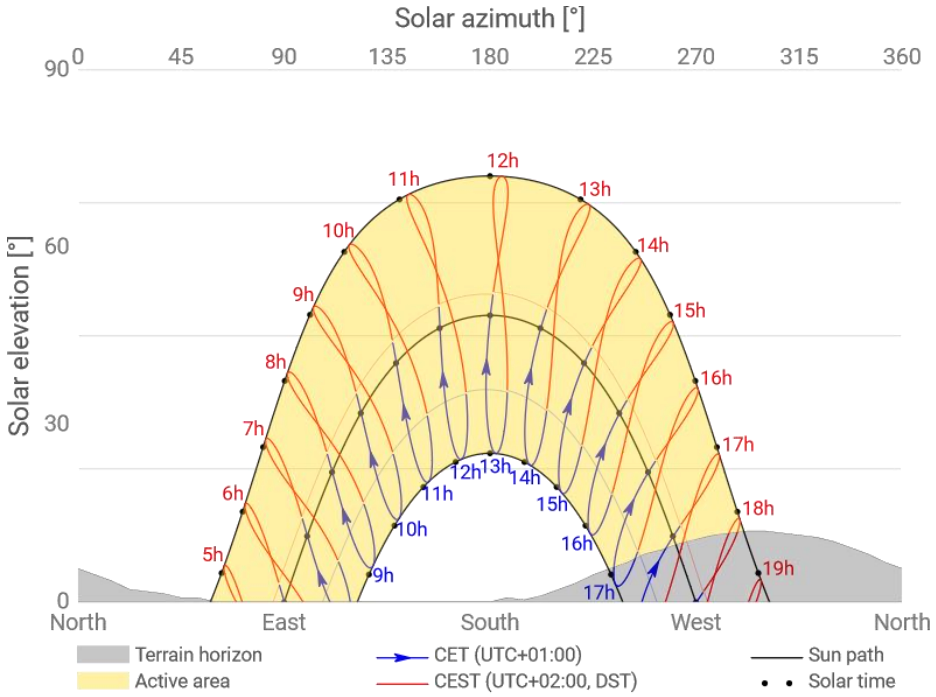

Figure 8 - Trajectories of the sun throughout the year and shade of the nearby hills [22].

A more detailed picture of the available solar resource can be found from the European Union’s PVGIS (Photovoltaic Geographical Information System) [23], from where hourly solar data of the requested location can be downloaded. These data include, amongst others, DNI (Direct Normal Irradiance), DHI (Diffuse Horizontal Irradiance), ambient temperature or wind velocity.

Other data, in this case related to the sun position, can be found at the NREL (National Renewable Energy Laboratory) [24], indicating amongst other information the azimuthal and

zenithal angle of the sun throughout the year. By using this data, the trajectories of the sun throughout the year can be plotted, as shown in Figure 9. The graph is very similar to the one shown above in Figure 8.

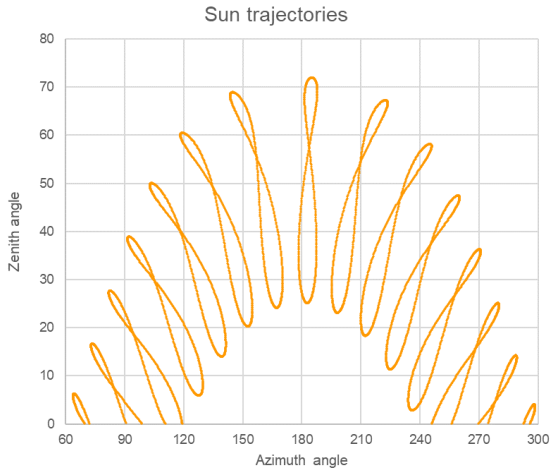

Figure 9 - Sun trajectories throughout the year.

An example of the solar data for a week may be found in Figure 10 below. The data represents de Global Horizontal Irradiation in the location for a week in April. As the graph shows, it seems to have been a cloudy or rainy week, with Tuesday or Thursday's sky completely clear whilst on other days the irradiation was far lower.

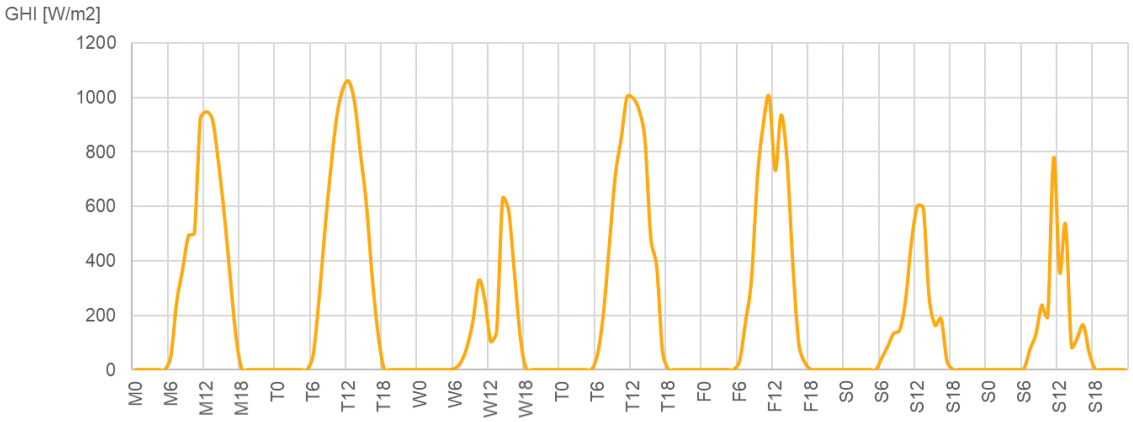

Figure 10 - Global Horizontal Irradiation on the location for a week in April.

3. Available technologies

3.1. Solar photovoltaic panels

Solar photovoltaic cells are electronic devices that allow electricity to be generated using solar energy. Given the reduced size, thus relatively low voltage and power output, they typically require to be connected with other cells in both series and parallel way in order to form larger modules. These modules are usually put together in the form of solar photovoltaic arrays which can cover areas as extensive as required [25].

3.1.1. Photoelectric effect

The physical principle to which energy transformation in this sort of cells is attributable is called photoelectric effect. This phenomenon occurs when photons collide with a material, supplying enough energy for this material to release electrons [26]. The amount of energy delivered to the electron must be higher than that of the band gap, that is, high enough to allow its transfer from the valence band to the higher-energy conduction band [27]. The band change of several electrons generates an electric current in the cell.

3.1.2. P-N junction

Solar cells are typically made of semiconductors (usually silicon), due to the low band gap that these materials present. Furthermore, in order to enhance electron transfer, the semiconductor is partly adulterated with trivalent atoms (P-doping) and partly with pentavalent atoms (N-doping), forming the so-called P-N junction [27].

The P-doped part, called acceptor, has a higher hole density (that is, more electron vacancies), whereas the N-doped part, called donor, has extra electrons. This way, the diffusion current is increased, since a higher number of electrons from the N part transfer to the holes in the P part, generating an electric field [27]. The behavior of solar cells is therefore much similar to that of a diode as, when applying a forward bias voltage, a net current from P to N appears.

3.1.3. The photovoltaic cell

The basic unit of solar photovoltaic energy generation is the solar cell. This component is based on a P-N junction, encased by an N-region, at the other side of which the front metal grid is located, and a much larger P-region, contiguous with the rear metal contact, as Figure 11 below shows. These contacts are connected electrically, therefore allowing electrons to travel through them.

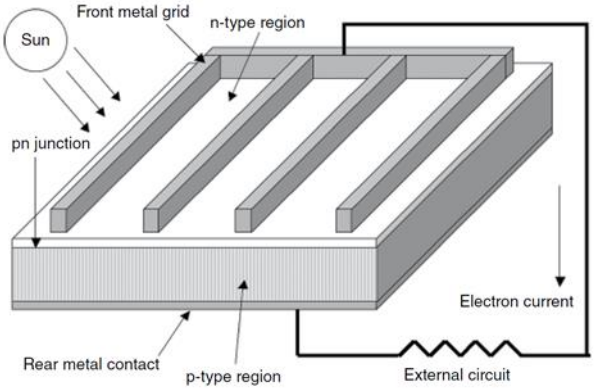

Figure 11 - Parts of a photovoltaic cell [28].

Once the photons reach the cell, their energy allows electrons to leap from the valence band to the conduction band, creating electron-hole pairs in the semiconductor material. The electron goes over the cable towards the rear contact, whilst the hole is transmitted towards it too, through the junction, and an electric current is generated.

In the case of silicon cells, which are the most common type of cells, each of these cells is capable of generating electricity at around 0.7 V peak voltage and can provide around 15 W of maximum power [29]. Since the number of cells in a panel varies on the model, usually between 36 and 144 cells, so does the output voltage of a commercial photovoltaic panel, as well as its rated power.

3.1.4. Structure of a PV panel

The structure of a solar PV panel is, in its sectional view, as Figure 12 below shows.

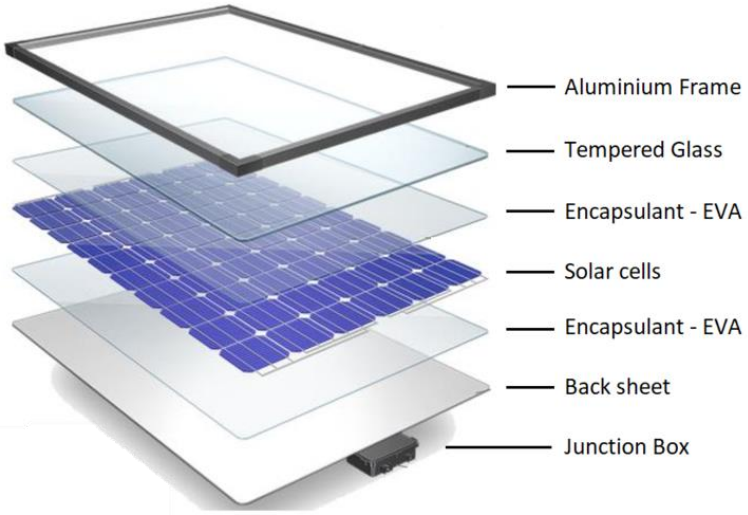

Figure 12 - Structure of a common photovoltaic panel [30].

The component located at the front of the solar panel, that is, the first part that sun rays reach, is a layer of tempered glass. This layer must be able to withstand harsh weather, as well as possible impacts on the panel caused by branches, animals, hail or any other origin [30].

The solar cells are enclosed in a thermoplastic material, being ethylene-vinyl acetate (EVA) one of the most common materials used for this purpose. This layer's objective is to protect the solar cells from vibrational, structural and thermal stresses in the silicon that would eventually lead it to failure by fatigue [31]. Furthermore, it blocks dirt and moisture from infiltrating towards the solar cells [32].

The back sheet is the posterior part also provides protection against any environmental agents that could physically or chemically damage the cell, besides granting insulation at the rear part of the panel [33]. Behind the back sheet, the junction box is located, which is the container of all electric items of the panel, and which must therefore present a proper insulation from the environment [34]. In the case of smart solar panels, it is also the place where electronic control devices are set [28].

3.1.5. Types of photovoltaic panels

There are several types of photovoltaic panels, the most common of which are nowadays monocrystalline and polycrystalline solar panels, which together represent around 95% of current photovoltaic production, according to a report by the Fraunhofer Institute [35].

Monocrystalline solar cells are composed by a single crystal of silicon, easing the flow of electricity and ensuring a higher efficiency. Meanwhile, multi-crystalline cells are made from many melt fragments of different crystals of silicon. Another, more visual difference is that monocrystalline solar panels have a uniform dark blue color whilst multi-crystalline panels show many fragments of different shades of blue which correspond to the different crystals [36], such as Figure 13 shows.

Figure 13 - Multi-crystalline (left) and monocrystalline (right) solar cells [37].

3.1.6. Arrange of solar panels

When installing the solar panels, the way they are connected is crucial in order to determine the output voltage and current of the array. If several panels are connected in series (in what is called a string), the voltage at which electricity is generated will be equal to the output voltage of a single panel times the number of panels. The current, though, will be the same no matter how many panels are connected in series. The main disadvantage of this configuration is that, when a panel is shaded, the whole string suffers the current decrease [38].

In a parallel connection, the opposite happens. The resulting current will be equal to the sum of currents of all panels, while the voltage will remain the same as the output voltage of a single panel. This way, if one or a few panels are shaded or malfunctions, the rest of the panels will be able to work normally [38].

Usually, photovoltaic panel arrays are arranged in several strings, preferably of similar characteristics, connected in parallel. This configuration allows to increase the voltage and current at which the energy is generated, and the shading of one or a few panels would only affect those panels in the same string, and not the rest of the array.

Regarding the orientation of the panels, they can be fixed to the ground in several different ways depending on its degrees of freedom. The cheapest way to fix them is at a fixed angle and facing South. This includes, amongst other solutions, to place them flat over the surface they are fixed to, to tilt them an angle slightly lower than the local latitude towards the South when aiming to maximize the yearly electricity generation, or to tilt them a larger even angle in order to maximize energy production on the day of the winter solstice [39].

One rotation angle implies that the panel may match either the sun's zenithal angle during the day, whilst facing South, or the sun's azimuthal angle along the local horizon, whilst having a fixed angle with respect to the ground. This sort of system is called a single-axis tracking system. As an example, at high latitudes, since the sun doesn't reach much altitude during an important part of the year, it is better to have the panels have the azimuthal angle rotation rather than the zenithal [40].

These solar angles are shown in Figure 14.

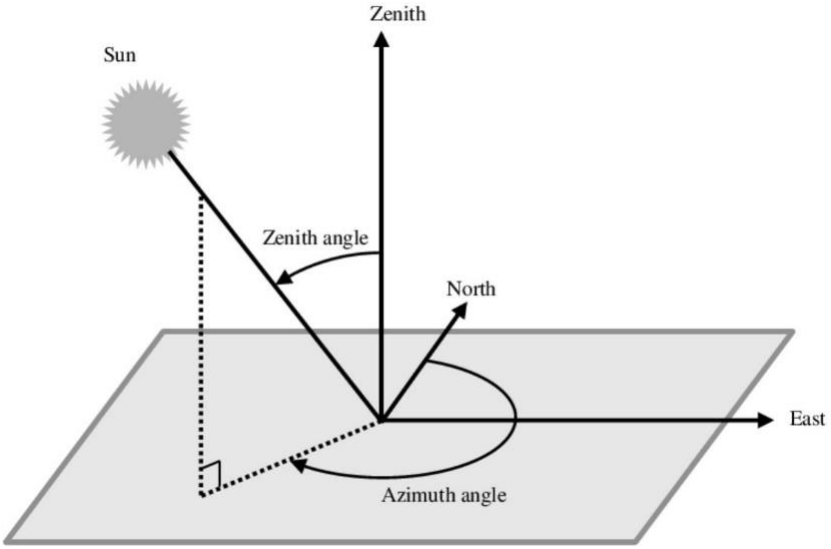

Figure 14 - Representation of the azimuth and zenith solar angles [41].

In the case of solar modules with two rotation angles, they are allowed to follow the sun's trajectory during the whole day, maintaining the panel perpendicular to sunrays at all time and optimizing the energy production. This kind of structure is called a dual-axis tracking system.

Logically, the more the panels can follow the sun, the more adequate the angle of incidence is and the higher the energy production. However, it will also require a higher cost of both installation and maintenance due to the complexity of the required tracking system.

3.1.7. Connectivity and electric components

In most photovoltaic systems, providing that the electrical energy obtained by the solar panels will flow as direct current, one or various inverters are required in order to transform this energy into alternating current. Inverters are one of the essential electrical components of a photovoltaic system, along with maximum power point trackers (from now on, MPPT). Inverters usually have a built-in tracker of this kind, which optimize the energy output, and both can be installed in several different configurations.

The most basic of the configurations where one or more trackers are included is to install a single, central inverter per tracker, that converts all the energy extracted from the whole photovoltaic array. This is the configuration which is cheapest and easiest to install, though it is also the least reliable of all. Another of the many existing arrangements would be, as an example, to install an inverter at the end of a string or of a few strings, which are afterwards connected to a tracker. The higher the number of inverters and trackers, the more expensive the system will be, nonetheless, its reliability against any possible failures, along with the output energy of the system, and therefore the efficiency.

3.1.8. Operation

Two of the most important parameters related to a photovoltaic panel's operation are the open-circuit voltage, which corresponds to the maximum voltage, and the short-circuit current intensity, which corresponds to the maximum current intensity. These two parameters are usually displayed in the voltage-current intensity graph of Figure 15 that describes the operation range of the panel, and that has the following aspect:

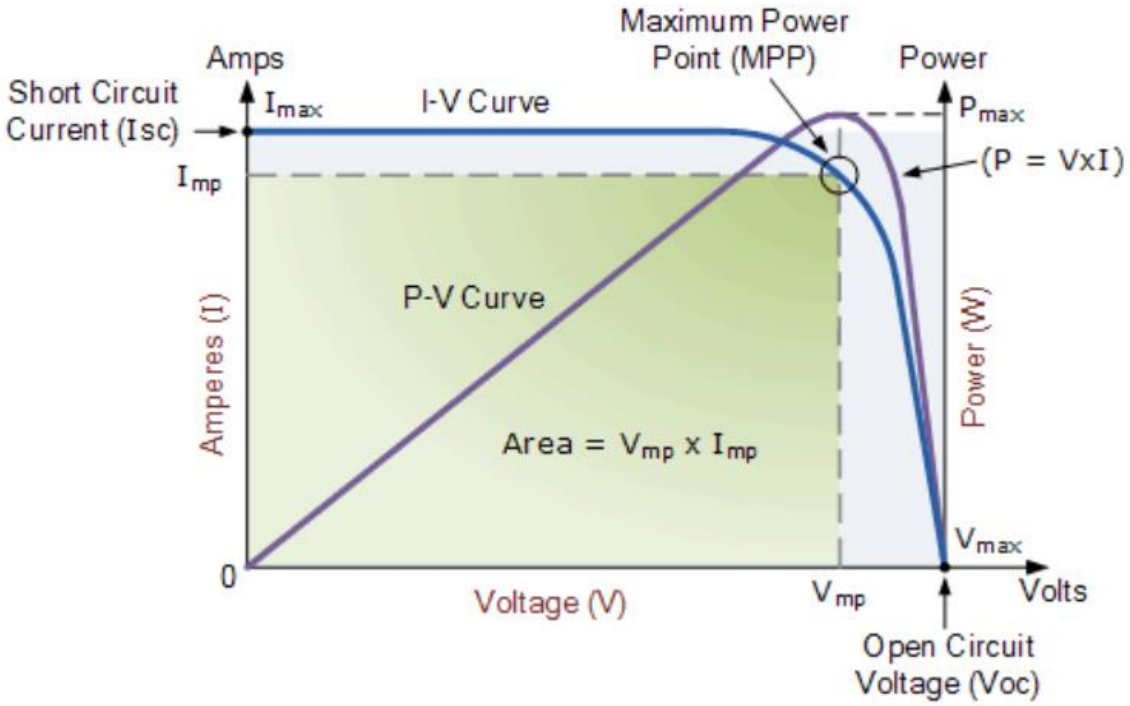

Figure 15 - Graph of the current and power provided by a photovoltaic panel as a function of voltage [42].

As the graph shows, the maximum power point is located at a point in the graph where both the voltage and intensity are slightly lower than their respective maximum values, and where they are called maximum power voltage and current intensity [42].

The graph showing power (as the product of the already mentioned voltage and intensity) is slightly different, being roughly triangular instead of roughly rectangular, as shown in Figure 15. The maximum power point is located at the upper vertex of the triangle and its value may be represented as P_{MPP}.

3.1.9. Efficiency

Regarding the efficiency of photovoltaic modules, it tends to be approximately 18-22% for modules based on monocrystalline silicon cells, though some of the latest modules have reached even higher efficiencies, being the maximum module efficiency in the market of

22.8%. For other kinds of photovoltaic cells, the efficiency is still below 30%, though for some experimental cells it is close to 50% [43]. However, and due to their cost, these cells are rarely used, only in applications that are either highly specific or have strong space restrictions, such as photovoltaic concentrators or for space vehicles [44].

3.1.10. Shade mismatch

An important part in the installation of photovoltaic panels is to consider the possible shading in these panels, whether it is from the environment (trees, buildings, mountains) or from other panels of the same installation. As an example, installing solar panels on the northern slope of a steep mountain may not seem a profitable investment at all.

The main problem that shading presents is that, once a cell is shaded, the current flowing through it will drastically drop, reducing the current in all its string of series-connected cells in the same amount. This implies that even a small shade in the panel may reduce its power output to half or less. Scaling this problem, if a panel is partially shaded, the rest of the panels in its string will suffer the same power output reduction, in consequence, it is crucial to analyze and avoid any shading in the panels.

3.2. Solar thermal

3.2.1. How it works

Another way of harnessing sun power is to extract it in the form of heat. In fact, even If photovoltaic panels pretend to extract electricity from the incoming energy, they will always heat up as well, making solar thermal power an attractive idea.

A cold heat transfer fluid enters the panel and flows inside metallic tubes that meander beneath the glass cover, gathering heat from the sunrays, which is transferred to the fluid. This behavior is analogue for panels that work with air or a mixture of water and glycol, which are the most common heat transfer fluids for these applications.

3.2.2. Parts

Most common solar thermal panels are composed by a handful of parts, each with a different purpose, as Figure 16 below shows:

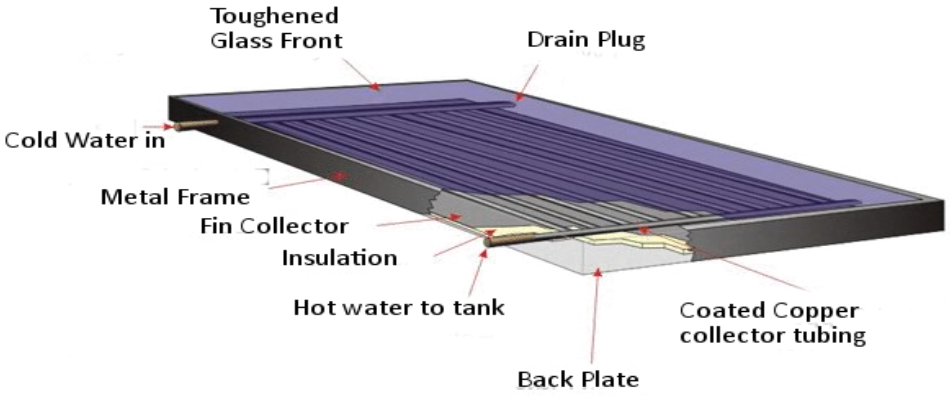

Figure 16 - Parts of a solar thermal panel [45].

3.2.3. Flat plates

In the first place, and similarly to photovoltaic panels, flat plate thermal panels are covered by a strengthened glass which can protect them from inclement weather or any object that may fall on them. At the same time, the glass' transparency allows sunrays to enter the panel in order to collect the energy they provide. It is also useful for the reduction of convection and radiation losses on the panel [46].

The tubes are located below this glass and are covered by a blackened surface which serves as a light absorber. These tubes lead either to their use place (a heating system, usually) or a thermal storage system, and are surrounded, except for the top part, by an insulator material, in order to minimize heat losses. Below this insulation, the bottom metal sheet is located, being its main purposes to protect the tubes and to fix the collector.

3.2.4. Low-temperature

This sort of panels are commonly flat-plate collectors, such as the one described above, their main application being the production of domestic hot water, though they are also used in space heating, air conditioning or the heating of other kinds of water. Since domestic hot water requires being heated at 60 ºC, these systems are often paired with an auxiliary system such as an electric heater, especially for winter months.

Low temperature thermal installations are mainly characterized by being comprised of a primary and a secondary water circuit, intertwined in a heat exchanger, pumps and a hot water accumulator [47].

The simplest sort of low-temperature solar thermal panels are air heaters, commonly used for indirect water-heating. In these panels, the fluid towards which heat is transferred is air, having as advantages respect to water its incapability of freezing or boiling, its non-corrosiveness or its null price. However, these ducts require more space and their leaks are harder to find than in the case of water [48].

It is important to notice that in solar thermal panels, unlike in solar photovoltaics, shading is not a severe problem. Obviously, the panels should be unshaded, but the temporal partial shading of a panel will affect if only slightly to the energy output and efficiency of the system. Regarding other considerations, this sort of panels (especially flat-plate due to their similarity) are installed taking into account the same variables as solar photovoltaic panels.

3.2.5. Medium-temperature

Medium temperature solar thermal collectors are usually heat pipe collectors, such as evacuated tube collectors, which operate at temperatures of between 80 ºC and 250 ºC. This sort of panels consists on the pipe containing the fluid being located into a void tube which induces a reduction on conduction and convection losses on the tube to around 5%, whilst in flat solar panels this convection is around 40% [49].

These tubes are located in parallel, with various of them connected on the top by the header pipe forming a panel [50]. This sort of tubes presents the structure shown in Figure 17, with an absorber surface which directs most of the collected heat towards the pipes inside the tube.

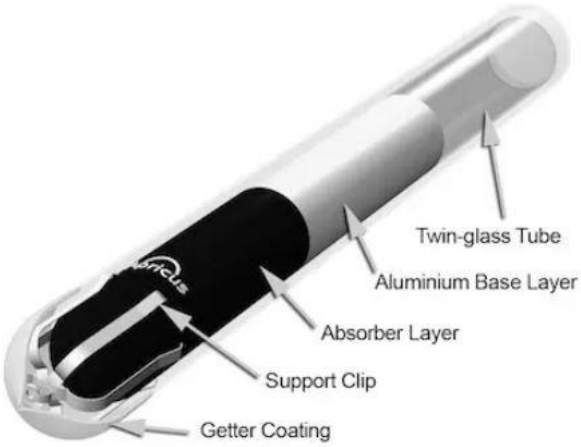

Figure 17 – Parts of an evacuated tube [51].

This sort of collectors presents many and diverse applications, including residential, commercial and process heating applications [52]. Other, less common applications are solar drying (either for wood or food), cooking (which is specially used in India) or water distillation for areas where drinkable water is not easily available [53].

3.2.6. Efficiency

The efficiency of solar thermal installations depends on the type of thermal collectors, though it is usually far higher than that of photovoltaic panels. In the case of flat thermal panels, their efficiency can even reach 90% [54].

3.3. Solar thermo-electric

Another way of harnessing the sun's energy is to concentrate the sunrays by means of a number of mirrors towards a line or point where a heat transfer fluid (HTF) is heated up, being able to reach temperatures far above 200 ºC. Subsequently, the high-temperature fluid is used to run a turbine, generating electric energy. Due to this sort of operation, high temperature solar thermo-electric plants are usually referred to as concentrating solar power (CSP).

There are several ways in which this concentration may be achieved, such as Parabolic Trough designs or Fresnel reflectors, though they are all based on the same principle: using parabolic-shaped surfaces with the aim of reflecting sunrays towards a linear collector located in the focus [55]. Central (or power) tower plants focus sunlight on a point at the top of a tower which stands in the middle of the many mirror structure. In this sort of plants, salt is molten so that it may be stored for several hours, allowing for electricity generation on demand, allowing for the plant to also generate electricity later during the night.

Another design is that of a dish connected to either a Stirling or a steam engine. This kind of thermal plants consists of a parabolic dish which reflects sunrays towards a point located at the focal point of the parabola.

High temperature collectors allow for energy storage, which may be done in different ways: as mentioned, it may be stored in the form of molten salts, a solution which may even allow a solar plant to produce electricity for 24 hours straight. Other options are steam accumulators, though their storage time is very reduced (close to one hour), or to store this thermal energy on graphite or in phase-change materials [53].

3.3.1. Parabolic Trough Collectors

The most common thermo-electric solar technology is Parabolic Trough Collectors (PTC). This sort of collectors consists on a parabolic metal sheet at the center of which a tube, normal to the parabola plane, is located. The position of this tube is exactly the position of the focal line of the parabola.

The way in which PTC work is the following one. In the first place, the collector has to be oriented sunrays reach the metal parabola in an angle parallel to its axis and bounce towards

the central tube, where the water can reach temperatures of around 400 ºC [42], or even a few thousand degrees, depending on the geometry of the mirrors and the collector tube.

The hot water (become steam by the time it exits the tube) is habitually used to feed a steam turbine through which the thermal energy is transformed into rotational energy, and by the action of a generator into electrical energy. At the exit of the turbine, there is always a low- or medium-temperature thermal energy byproduct which, since these big solar plants are usually located far away from cities, tends to be used to cover the plant's thermal energy needs.

Since the sunrays must always be parallel to the axis of the parabola, PTC solar panels require a two-axis tracking system, in order to follow the sun's path throughout the day and for each day of the year.

For this sort of energy collectors, the thermal efficiency can reach up to 75% efficiency [56], though it is important to notice that the overall efficiency needs to take into account the efficiency of the turbine and any thermal or electrical losses of the energy transformation, lowering the overall efficiency to around 15% [57].

3.3.2. Efficiency

The efficiency of the electricity production by these technologies ranges between 11% and 16% for parabolic trough, around 13% for linear Fresnel, between 7% and 20% for solar towers and between 12% and 25% for dish Stirling, according to the International Renewable Energy Agency (IRENA) [58].

3.4. Solar hybrid

In the field of solar energy, there is yet another technology that allows both thermal and electrical energy harnessing from sunrays. This is the case of hybrid (photovoltaic-thermal) solar energy.

This technology works essentially as a conventional PV panel with an added heat-collecting system (underneath the PV layer) which not only allows the extraction of thermal energy, but also cools down the PV panel, increasing its efficiency. A hybrid solar panel consists of the parts shown in Figure 18:

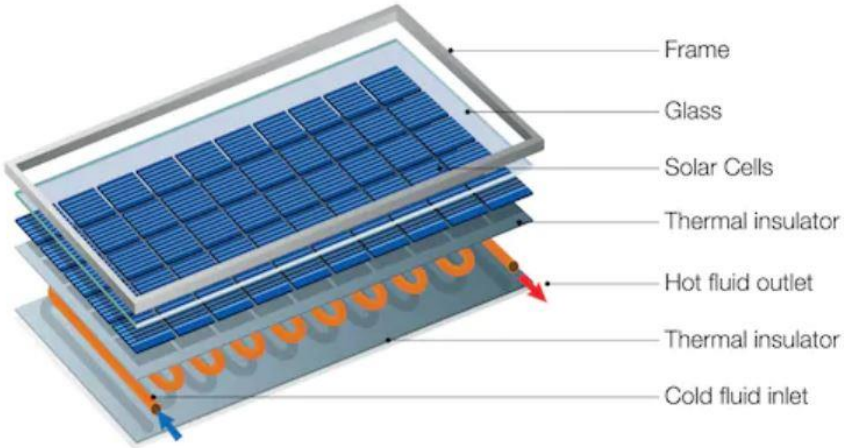

Figure 18 - Parts of a solar hybrid panel [59].

3.4.1. Structure of the PVT panel

Photovoltaic-thermal solar panels are formed by several layers of different materials, the outermost of which is an anti-reflective cover glass that provides protection against any possible impacts that the panel may suffer. Additional glazing layers may also be placed on top of this glass for a further reduction of convective and/or radiative energy losses [60].

This glass is located directly on top of the ethylene vinyl acetate (EVA) layer, which avoids the degradation of photovoltaic cells due to environmental agents such as moisture or dust, as well as from other inclement weather.

The photovoltaic cells are located below the aforementioned protections and fixed to a metal sheet. These cells work in exactly the same way as in a photovoltaic panel, with only one slight difference: whilst photovoltaic panels tend to overheat and therefore to reduce their efficiency, especially during summer, on hybrid panels this metal sheet absorbs part of this heat and conducts it towards fluid-conducting tubes located below.

The tubes are surrounded, except on top, by insulating material, in order to ensure that as much heat as possible is being transferred to the fluid. This way, the heat that escapes the photovoltaic cells into the underneath tubes accomplishes two functions: it prevents, or mitigates, the overheating of the photovoltaic cells, whilst serving for more energy production in the form of thermal energy.

The explained tube configuration is for the most common PVT panels, though in certain air-heating PVT panels, the air passes above the photovoltaic cells, or even both above and below, either in parallel tubes or as part of the same tube where the air passes twice through the cell [61].

3.4.2. Arrange

The most common ways to arrange hybrid solar panels don't differ from the way in which the photovoltaic panels are arranged, so these ways have already been explained in 3.1.6. The same happens with their connection, since a PVT solar cell is essentially a photovoltaic cell with the advantage of using part of the received heat to harness as thermal energy.

3.4.3. Types

There are different types of PVT panels, depending on their geometry and on the fluid they heat. Some panels provide domestic hot water, while others work at medium temperature and allow for electricity production. Some of the liquids used for this sort of panels are water, mineral oil or glycol [62]. Other PVT panels use air as their heating fluid, and are therefore appropriate for heating, ventilation and air conditioning systems.

3.4.4. Operation and efficiency

The combined efficiency (electric plus thermal) of PVT panels tends to be higher than that of photovoltaic and thermal solar panels. Depending on the type of the photovoltaic cell, the fluid and the overall structure of the panel, electrical efficiency may rise between 15 and 20%, being practically the same or slightly lower than that of a photovoltaic cell of similar characteristics.

On the other side, some PVT panels are capable of reaching a 50% or higher thermal efficiency, though the PVT panels with a higher thermal efficiency are usually those with an electrical efficiency that doesn't usually surpass 10% [61].

3.5. Connection systems

There are two main ways to connect a renewable power plant such as solar photovoltaics, depending on whether their operation is independent from the grid (stand-alone energy systems) or if they operate while connected to it (grid-connected energy systems).

Stand-alone energy systems are mostly used in remote, isolated areas. These systems need to be capable of matching the demand at all times, which implies that they need storage systems in order to ensure that energy is available at any time, increasing the cost of the system. This is especially so for renewable sources, which are not available on demand [63].

However, these inconveniences imply that during peak production hours some energy may go to waste if the storage system is already at full capacity. In the case of solar-based systems, that could be, as an example, in July if the weather is sunny for a few days in a row. Moreover, in rainy winter days, there could be no energy available, which is why this sort of systems are usually combined with a gas or oil generator [63].

On the other hand, grid-connected energy systems offer the versatility of being able to cover the demand at all time by using energy from the grid when needed, whilst the energy surplus may be sold to the grid. This way, solar photovoltaic or wind energy installations that are connected to the grid don't require an energy storage system.

In the studied case, the hospital's energy consumption needs to be guaranteed at all times, and it's located in the center of the city, with easy grid connection available. Additionally, due to the high energy density required by the hospital, the installation is not expected to cover the hospital's energy demand. It is for these reasons that the installation should be connected to the electrical grid.

3.6. Storage systems

Energy storage plays a vital part in energy systems. This sort of systems is especially useful in the case of a system failure, when the storage systems may provide energy until the fault is over. For installations based on renewable energy, such as solar energy, which is highly variable depending on the weather or the time of the day, these storage systems may supply energy to cover the night or cloudy days' demand.

3.6.1. Electrical batteries

Since electricity can't be stored, energy must be stored in other forms, such as chemical, mechanical or thermal energy. One of the most common and efficient ways to store electrical energy is in the form of chemical energy, such as lead-acid, nickel-cadmium or lithium-ion batteries, amongst other technologies.

- Lead-Acid batteries

One of the most common types of batteries in the market are lead-acid batteries, whose main advantage is their low cost per watt. They are also more robust and reliable than other sorts of batteries, are able to supply high current and are available in a wide variety of capacities and sizes [64]. Lead is also one of the most recyclable materials, and in the EU almost 100% of lead-based batteries are recycled [65].

However, the life of these sort of batteries is quite short, usually between 300 and 500 cycles, and are not apt for fast charging. Another inconvenient is their large size and weight, which makes them impractical for small or compact applications [64].

- Lithium-Ion batteries

Another of the commonly used types of batteries are lithium-ion, which are used in many applications, such as mobile phones or laptops, or hybrid and electric cars. This sort of batteries excels in energy efficiency, lifespan, compactness and scalability, and require no maintenance [65].

The manufacturing of these sort of batteries (and therefore its price in the market) is more expensive than other batteries such as those made of Nickel and Cadmium [66]. However, their price has been decreasing significantly over the past decade, and by 2018 their cost was around an 85% lower than in 2010, as Figure 19 shows.

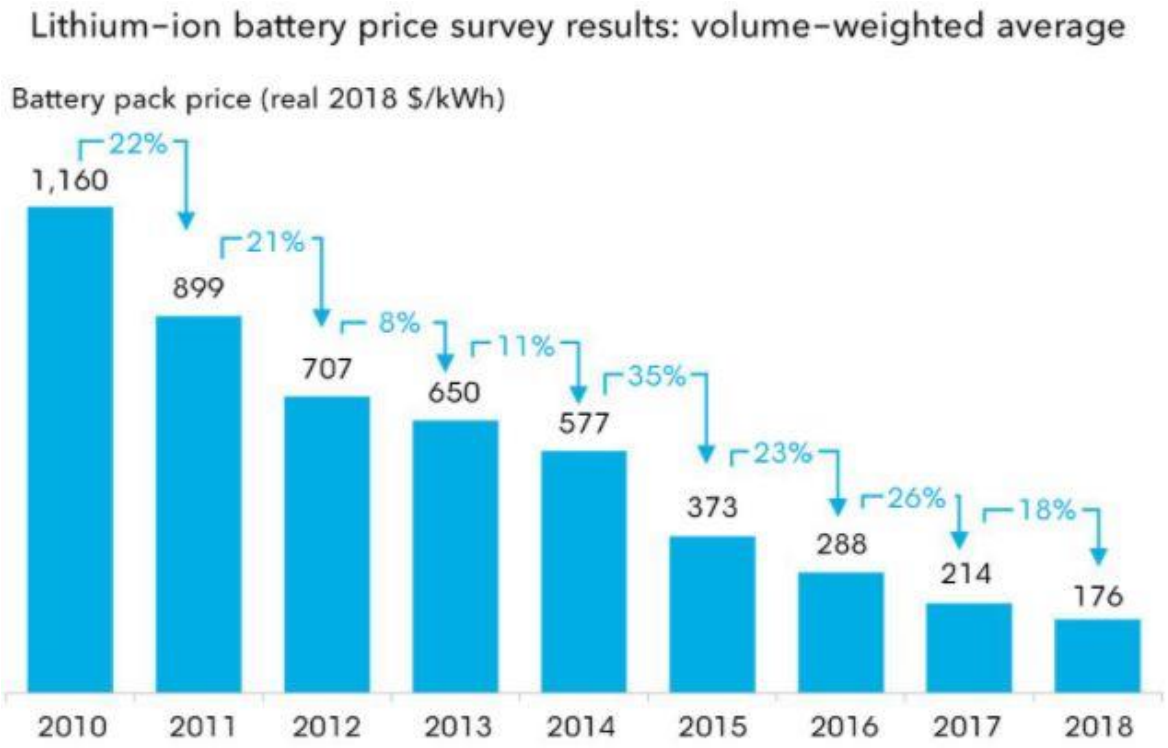

Figure 19 - Evolution of the price of lithium-ion batteries (2010-2018) [67].

- Nickel-Cadmium batteries

Nickel-Cadmium batteries are a cheap sort of batteries available in many shapes and sizes which are able to charge and discharge fast, operate at a high temperature range and have a relatively long lifespan. However, they also present some inconvenients, such as the toxicity of its components and its low energy density [68].

3.6.2. Thermal storage

Another way of storing energy is in the form of heat kept in a material in order to be released when needed. This sort of storing is usually more effective on the short or medium term, since on the long term the thermal losses decrease the efficiency of these storage systems. This energy is usually stored as either sensible heat, latent heat or in a thermo-chemical form [69].

- Sensible heat storage

Sensible heat thermal energy storage systems are usually based on water due to its low price, high specific heat capacity and number of applications, both domestic and industrial. It is a good option to use alongside solar thermal panels, since the energy surplus generated at midday may be stored for its use at night. This way, a solar installation could provide energy even at times when there is no sun.

This technology is sometimes used on a large scale, with several thousand cubic meter hot water tanks as a seasonal storage combined with small district heating systems. The tanks used for this sort of applications may be based on underground heat or cold-water storage systems, whether in an aquifer, a pit or other sites [69].

The storage efficiency of this technology ranges between 50% and 90%, and it may be improved by reaching a highly effective insulation and water stratification. Its capacity is not as high as that of the other technologies, but it is the cheapest one, with a cost of between 0.1 and 10 €/kWh depending on various factors such as its application, size and insulation [69].

- Latent heat storage

Another way to store thermal energy is in phase-change materials, which have a higher storage capacity than sensible heat storage systems since they also use the latent heat of the material. This sort of materials may be used for heating or cooling and in average reach higher storage efficiencies than sensible heat systems (between 75% and 90%) [69].

Some solar tower or similar concentrating power plants use the high temperatures reached at the central collector to melt salts with a melting point of around 300-500 ºC. These phase-change materials allow for a large production of energy by boiling water for the production of electricity through a Rankine, Brayton or similar cycle. Molten salts have, though its high melting point, an also high specific heat capacity, so they are able to store large amounts of energy for a few hours or days. [70]

The energy density of latent heat storage systems is also far higher than that of sensible heat systems, being one of the main advantages of these systems. Their major drawback is the cost, being between 10 and 50 €/kWh, partly due to the heat transfer technology that needs to be able to reach a high charging and discharging power [69].

- Thermo-chemical storage

Thermal energy (both heat and cold) can be stored in the form of some thermo-chemical reactions like sorption on microporous or composite. This method allows the desorption, then transportation of thermal energy and the adsorption at the discharge site, with a very high energy density and also a high efficiency. A schematic of the operation of this sort of systems is shown in Figure 20 [69].

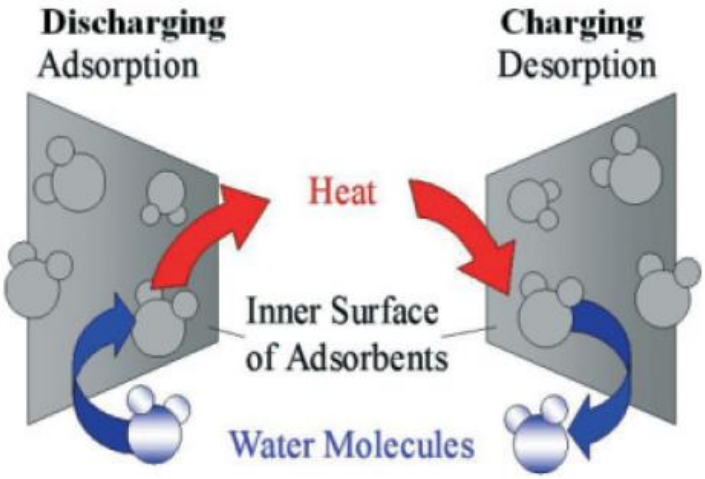

Figure 20 - Thermo-chemical storage system operation schematic [69].

These systems are also able to convert heat into cold at the same time that they store thermal energy. However, this is a more complex technology than sensible heat storage and its costs tend to be far higher, at between 8 and 100 €/kWh [69].

4. Load description

The following step is to characterize the load of the hospital, both in electrical and thermal energy. For this purpose, the data of the annual electrical and thermal loads were obtained directly from the hospital, where the thermal load is supplied by burning natural gas. These energy consumptions are the ones shown in below:

Table 1 - Electricity and natural gas yearly consumption at the hospital.

Electrical load	40,890,758 kWh_e
Thermal load	1,122,079 kWh_{th}

4.1. Electrical load

Regarding the electrical load of the hospital, due to the lack of more detailed data, the consumption of a hospital in *Comunidad de Madrid* in 2015 as described by Pedrajas [71]. Pedrajas details the monthly consumption of the hospital, as well as the hourly consumption for an average week. These data could be used to extrapolate a load curve of a hospital and obtain an estimated load curve for Hospital de Sant Pau.

The first step was to calculate the actual monthly consumption, which are shown in Table 2:

Table 2 - Electricity consumption per month.

Month	Load [kWh_e]
January	3,333,988
February	2,810,292
March	3,102,922
April	3,230,887
May	3,357,586
June	3,656,430
July	4,215,156
August	3,953,564
September	3,456,845
October	3,451,627
November	3,332,027
December	2,989,435
TOTAL	**40,890,758**

Afterwards, the hourly consumption throughout an average week was expressed as percentages of the whole week's load. This way, the percentage of consumption that each day represents regarding the week's total load can be obtained. With these data, the hourly power consumption profile throughout a week could be found for each month. The profile of the average week is then the one shown in Figure 21.

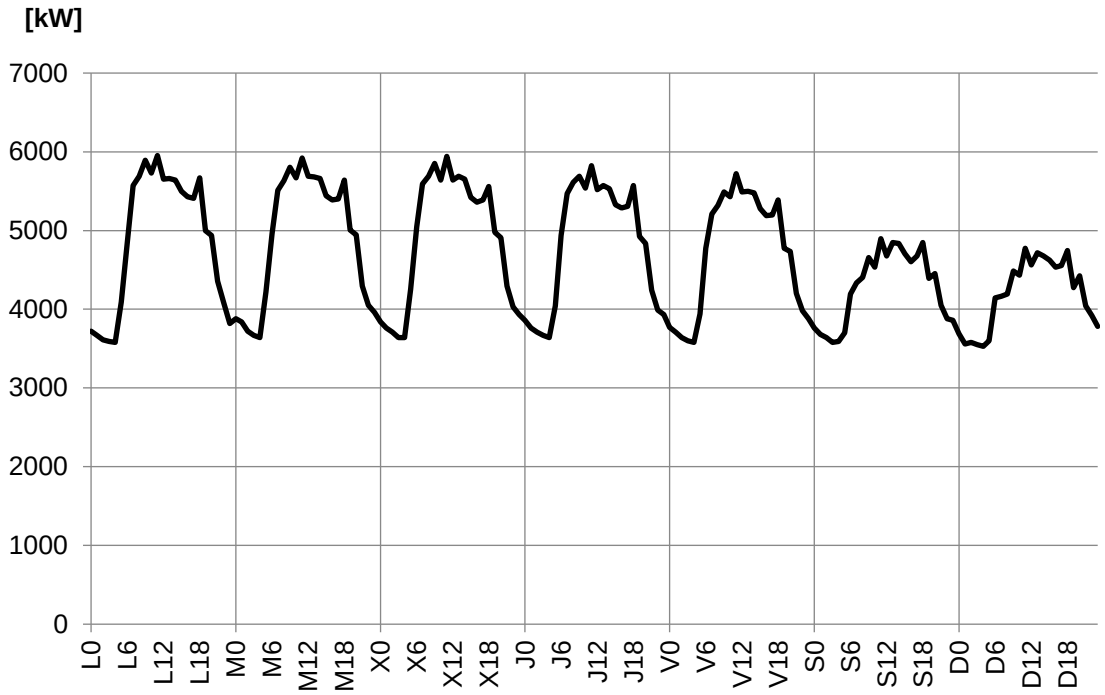

Figure 21 - Average hourly power consumption profile of Hospital de Sant Pau.

In the horizontal axis of the graph (and of the following graphs) the letter is the initial of the day of the week, whilst the number is the hour of the day.

This calculation took into account the fact that every month has a different length, and that the consumption varies depending on the day of the week (the most remarkable of these differences being the decrease of electricity consumption during the weekend). Therefore, and since that the data obtained from Pedrajas [71] corresponds to year 2015, January is considered to begin on a Thursday and end on a Saturday for the calculations, doing similarly for the rest of the months. This way, at the same time as the length of the month was considered, so was the consumption drop on weekends.

The result of the aforementioned calculations can be shown for each month in Figure 22, Figure 23, Figure 24 and Figure 25. For the sake of clarity in the graphs, each graph shows only one season, as well as the average week in the whole year so that an easy, visual comparison can be made.

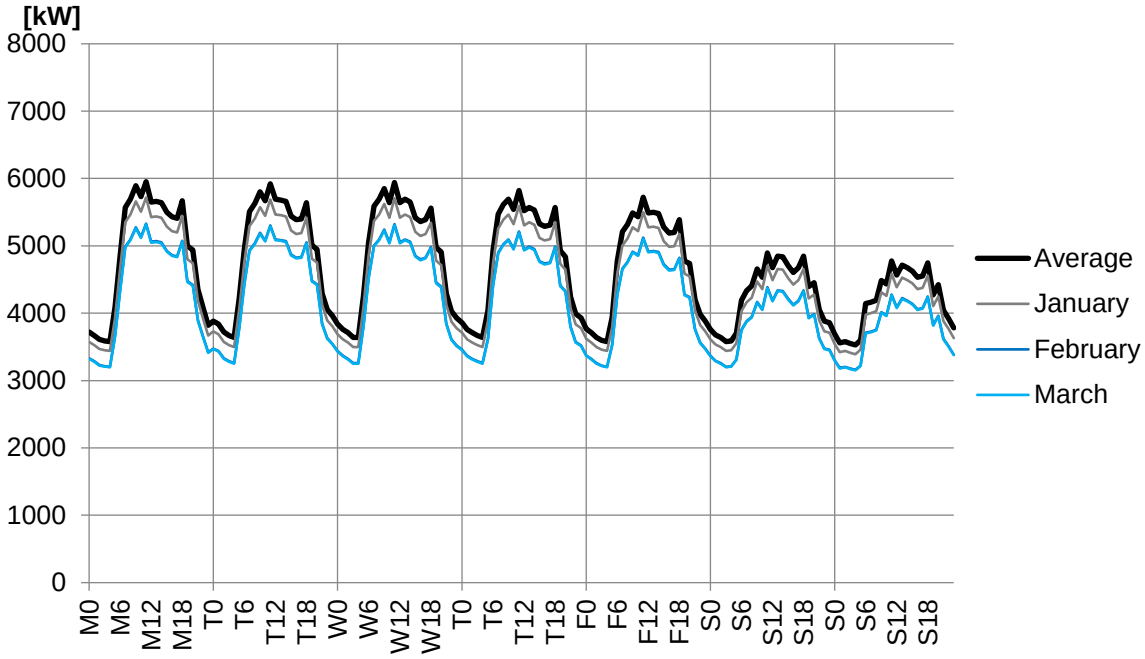

Figure 22 - Average hourly power consumption profile of Hospital de Sant Pau (winter).

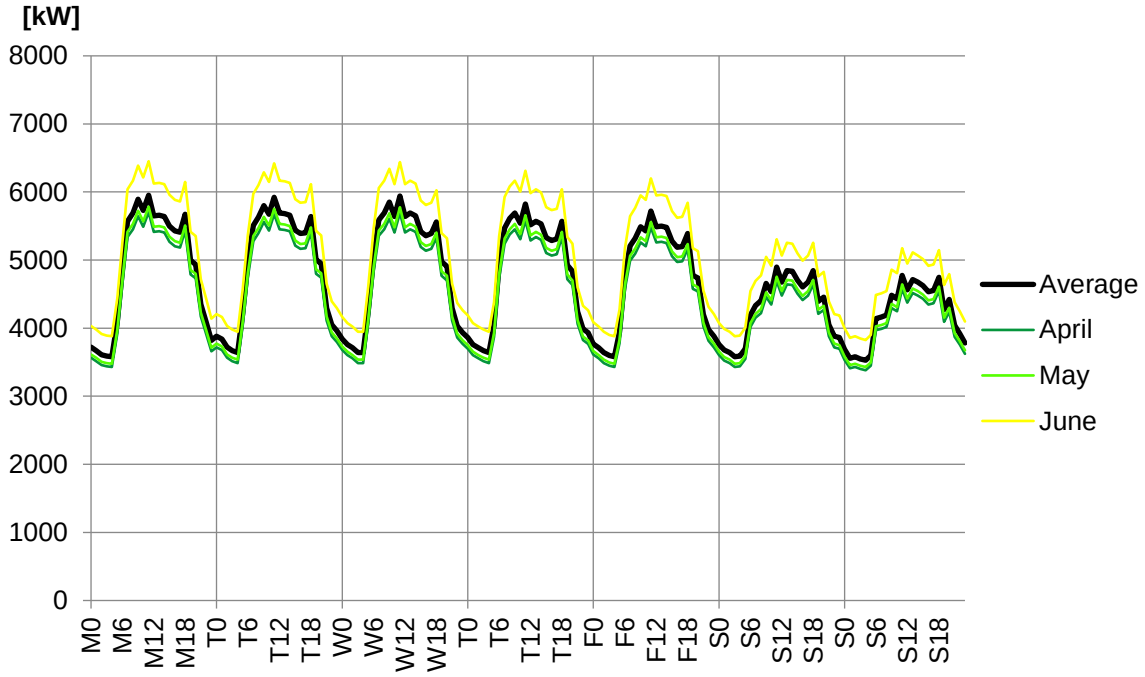

Figure 23 - Average hourly power consumption profile of Hospital de Sant Pau (spring).

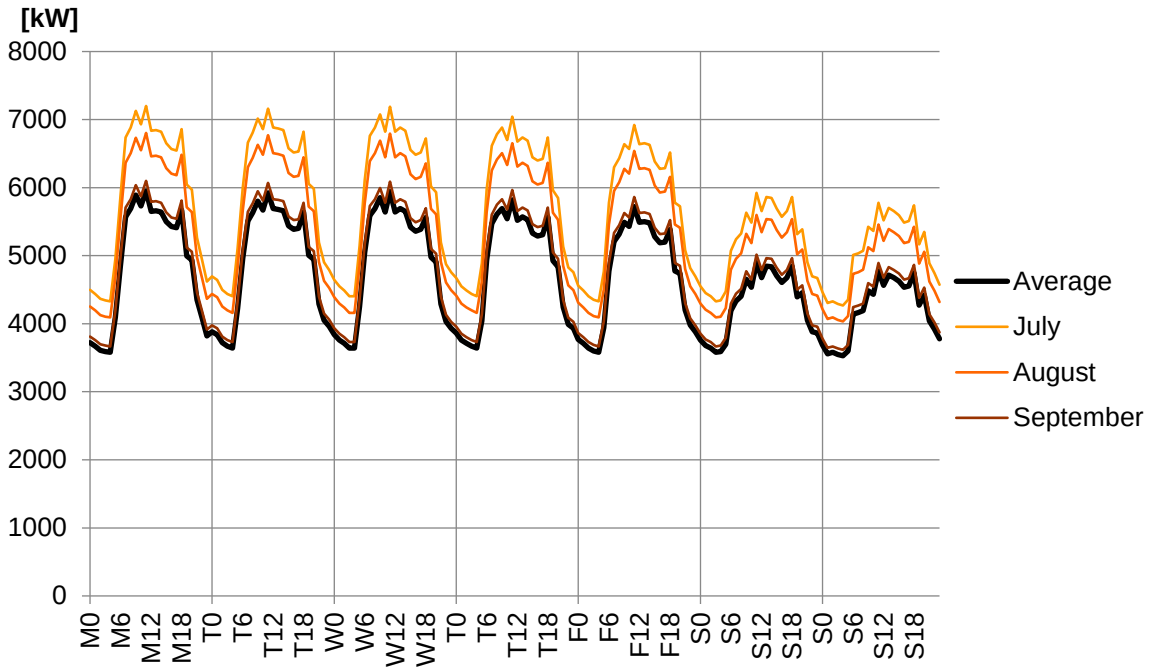

Figure 24 - Average hourly power consumption profile of Hospital de Sant Pau (summer).

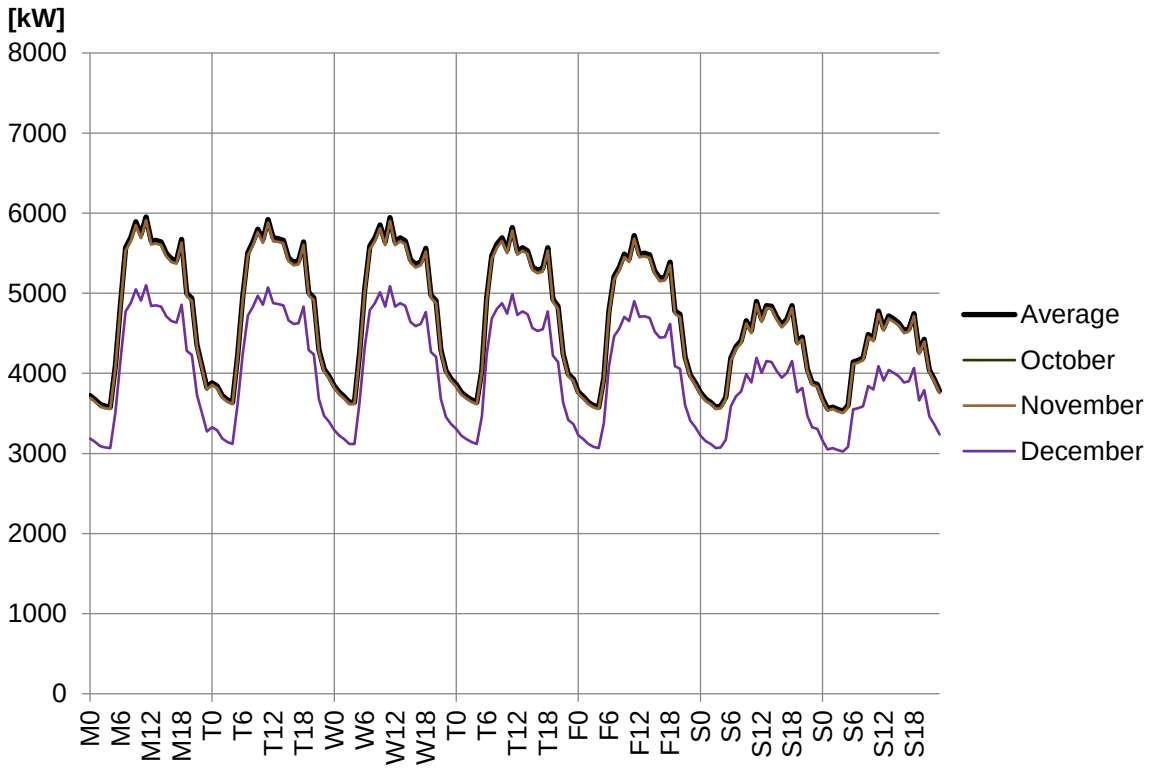

Figure 25 - Average hourly power consumption profile of Hospital de Sant Pau (autumn).

The graphs show that the average consumption is significantly surpassed only in three months: June, July and August. In September, the consumption is also above average, but only slightly, and in the rest of the months it is below average.

When it comes to the analysis of each day, it is important to notice that the electricity consumption never drops to zero, being its minimum value at dawn and around two thirds of the common consumption during the day. During weekdays, there is a peak in the morning, between 9 and 11 h and a slightly lower peak around the evening, between 18 and 20 h.

At weekends, the night consumption remains approximately the same as during weekdays. During the day, though, the load is significantly lower, decreasing slightly on Thursday and Friday and more steeply towards the weekend, being the consumption of a Sunday around 19% lower than that of a Monday. The peaks are presented at the same hours, though the valley presented in the early afternoon of weekdays is less deep.

4.2. Thermal load

In the case of the thermal load, there was no consumption profile available; the only known data was that the natural gas consumption is 1,122,079 kWh per year. However, this amount of energy doesn't correspond to the global thermal energy demand, since the ratio between electrical and thermal demand established by Mínguez [72] suggests that the thermal consumption of the hospital is around 12.75 GWh. This implies that the thermal energy consumed by the hospital is expected to be covered in around a 90% by electricity (such as electric boilers) and not only by natural gas.

Due to these reasons, and with the few data available, the thermal demand profile has been assumed to have the same shape as the electricity demand profile. The profile for natural gas consumption has also been assumed to present the same shape, which would be approximately like the one shown in Figure 26, for an average week.

The graph shows that except for a few hours throughout the week, the gas consumption is above 100 kW and doesn't exceed 160 kW. The gas consumption is higher during the day, and higher on weekdays than on weekends.

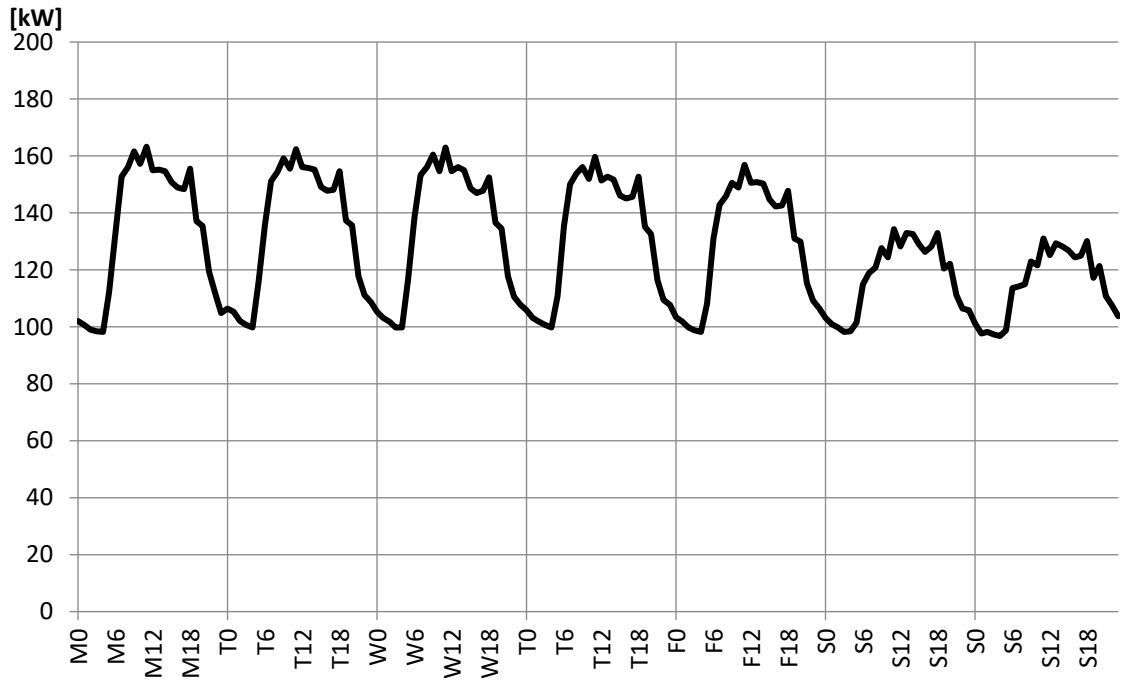

Figure 26 - Average weekly gas consumption at Hospital de Sant Pau.

5. Installation sizing and design

In this chapter, various energy-harnessing options are analyzed and calculated in order to meet the energy requirements explained in chapter 4. These options, all based on solar energy, are the following ones: an installation based on photovoltaic panels, another based on thermal panels and a third one based on hybrid photovoltaic/thermal panels.

5.1. Available area

The first thing that needs to be known in order to dimension the installation is the available area in which the panels can be installed. With this purpose, the various roofs of the hospital were analyzed, considering whether they were suitable surfaces as to place a solar installation.

The area of the different roofs which presents adequate characteristics was calculated, considering the shades that could appear during the day. In order to simplify the calculations, the shade was considered as if the sunrays were always coming from the southward direction. This will imply that, if an obstruction was placed at the Southwest of one of the roofs, the amount of energy calculated for the morning hours will be lower than the actual one, but in the afternoon the effect will be the opposite. In any case, the slight global difference throughout the day will be neglected.

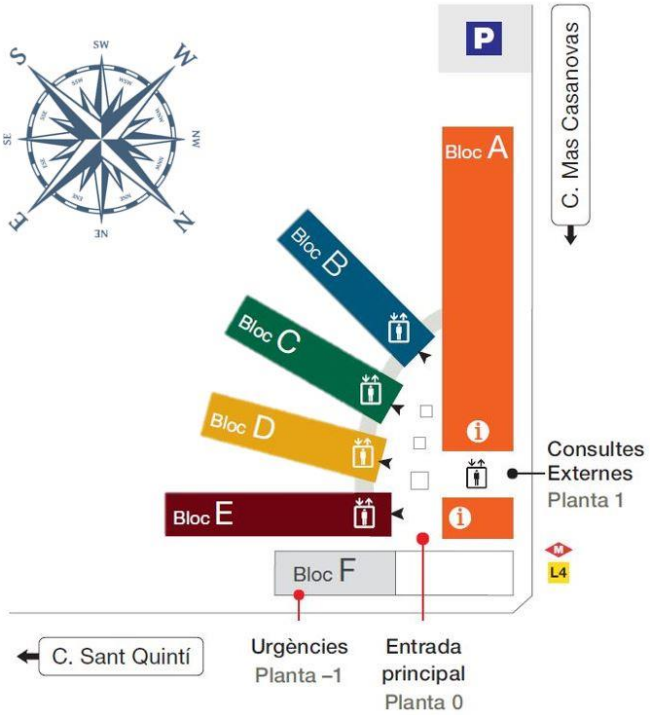

Figure 27 - Blocks of Hospital de Sant Pau [73] [74].

The new building of the *Hospital de Sant Pau* is divided into several blocks, named A to F as shown above in Figure 27.

Block A faces roughly Southwest, Block B is extended towards the South, each of the blocks C, D and E is deviated 15º more towards the East than the previous one, and block F is parallel to block E and perpendicular to block A, facing then towards the Southeast.

The available roof areas have been then sketched and measured, using industrial drawings provided by the Hospital, and obtaining the following areas:

Table 3 - Area of the available surfaces.

Surface	Area [m²]
A1	1,364.0
A2	613.7
A3	422.7
A4	745.7
B1	523.6
B2	176.7
C1	523.6
C2	176.7
D1	523.6
D2	176.7
E1	446.3
E2	176.7
F	N/A
TOTAL	**5,870 m²**

These areas are sketched (approximately) in Figure 28.

Figure 28 - Distribution of the available surfaces.

5.2. Photovoltaic modules

In order to determine the power output in detail, the first calculations to make were to estimate the percentage of the surface that may be covered by panels. This was calculated in detail for the parts B1, C1 and D1.

To begin with, the optimal separation between two rows of panels was found for area B1. This area faces south, making it easier to study, since all rows will have the same number of panels and will be perfectly aligned. The separation between rows needs to be considered, since their 38º inclination may cause the rows behind to be shaded. The panels will be fixed, and always facing South.

Calculations were made following the guidelines of *Urrutiko Lanbide Heziketarako Institutua* [75] and considering that as soon as part of the panel is shaded, the whole panel (and the rest of its row) are fully shaded. This was assumed since once a panel is partially shaded, its productivity drops drastically. Thus, once this happens, the output power was calculated for only the first row of panels.

Figure 29 below shows the main parameters to be calculated regarding row separation. The parameters l, h and s' are already known, so s (and thus d) were calculated for several values of α. The aim of these calculations was to represent graphically the variation of the output energy (both in total and per panel, which represents an approximation of the energy output per amount of money invested) as the distance between rows d. With the first calculations, the candidates to optimal points were found to correspond to α angles of around 22º, so instead of calculating in 2º intervals, between 18 and 26º, the intervals are of 1º for the sake of a better optimization. All calculations are made considering a full year.

Note that Figure 29 has some actual numbers, but they are only examples and not the

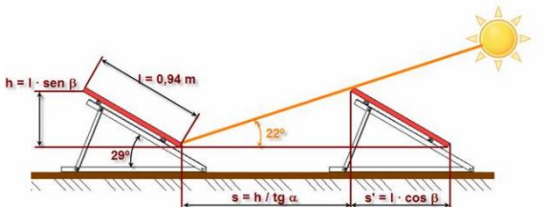

Figure 29 - Calculation of the separation between rows [75].

numbers with which calculations were performed.

Since the output power is expected to be far lower than the hospital's consumption at all times throughout the year, the aim of the calculations was to maximize the total energy output, though also considering the productivity of the panels. This means that, as an example, if 8 rows of panels were to produce only slightly more energy than 7 rows would, installing 7 rows would be considered a better option due to the significantly higher amount of energy produced per euro invested. This criterion is also ecological, since less panels would need to be produced for roughly the same energy output.

Moreover, two options were studied: whether the panels should be installed with the long side of their rectangular shape horizontal or with the long side "vertical" (that is, inclined 38º as mentioned, not really vertical). For simplicity's sake, these orientations will be referred hence as "horizontal" and "vertical" respectively. In both of the cases, a space (typically ranging from 1 to 2 m) was left as an aisle for maintenance purposes, since the rows are oriented perpendicularly to the entrance to this roof. The panel chosen for these calculations was SunPower Maxeon 3.

The calculations for area B1 show the following results (see Figure 30). The parameter d is graphically explained in Figure 29.

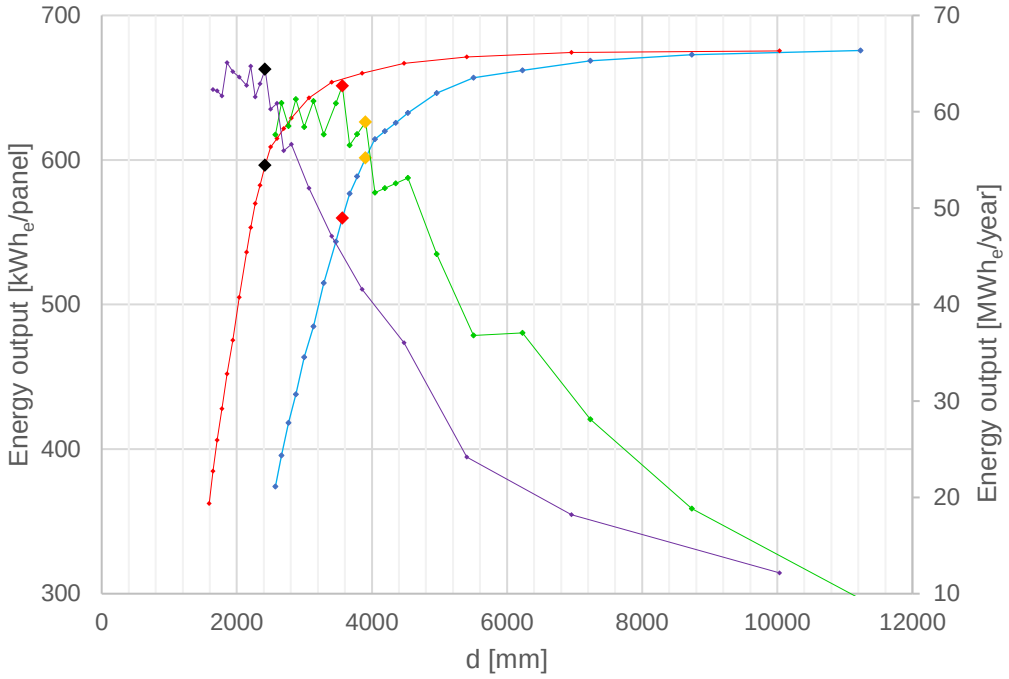

Figure 30 - Energy output (total and per panel) at surface B1 versus the distance between two rows (d).

Where:

- Blue line: power output per panel (vertical panels).
- Green line: total power output (vertical panels).
- Red line: power output per panel (horizontal panels).
- Purple line: total power output (horizontal panels).

In Figure 30, each pair of colored diamonds represent one of the main candidates to optimal point. Regarding panel productivity, the yellow points (corresponding to vertical panels) and the black points (corresponding to horizontal panels) present a similar value, and far higher than the one presented by the red points. Out of these two options, the black points present a significantly higher total energy output, which is the reason why it was considered the optimal solution.

Hence, the best option appears to be to install 12 rows of 9 panels each (that is, a total of 108 panels), separated around 2.42 m from one another, that is, with a limit incidence angle of 22º. There is a 1.79 m wide maintenance aisle which can be located either at a side of the rows, or in the middle, dividing each of them in two sub-rows of 5 and 4 panels each.

For blocks C1 and D1, the calculations followed the same steps, with two slight considerations. Firstly, these blocks do not face south, they are inclined 15º and 30º respectively towards the Southeast. Thus, the width available for the rows is slightly

different: a straight East-West line would have a length of 17 m (the width of the block) divided by the cosine of 15º and 30º respectively. A line of panels, however, will have a slightly lower length, since the depth of the row (variable s' in Figure 29) also needs to be taken into account.

Secondly, there will not only be space for a number of "full" rows (expected to be lower than on block B1), but also for additional shorter rows located on the Northern and Southern corners of the block, as shown in Figure 31.

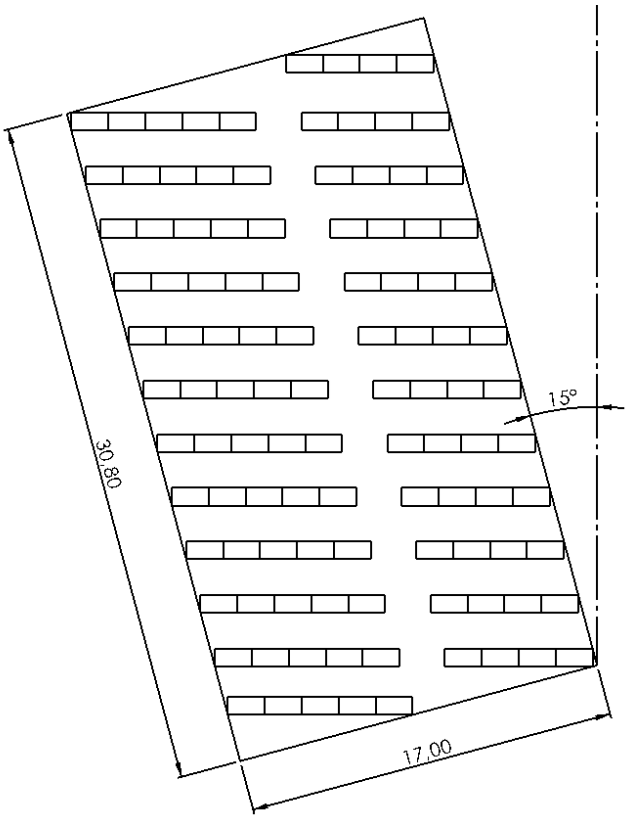

Figure 31 - Layout of the photovoltaic panels in block C1.

Calculations were performed analogously to those of block B1 but considering only the "full" rows. Then, the number of panels in additional shorter rows was obtained, considering the row separation of the best solution. Finally, considering this number of extra panels, final calculations were conducted.

It is important to note that this number of "extra" panels was considered to be the same in all cases for the sake of simplicity. This decision may prove unfair for the most extreme configurations (the ones with a higher row separation present an unreal advantage towards those with a lower separation). However, these extreme configurations are not even close to be optimal candidates, because of a low overall production and low productivity respectively, so this decision doesn't really affect the results.

The results found for C1 are the ones shown in Figure 32.

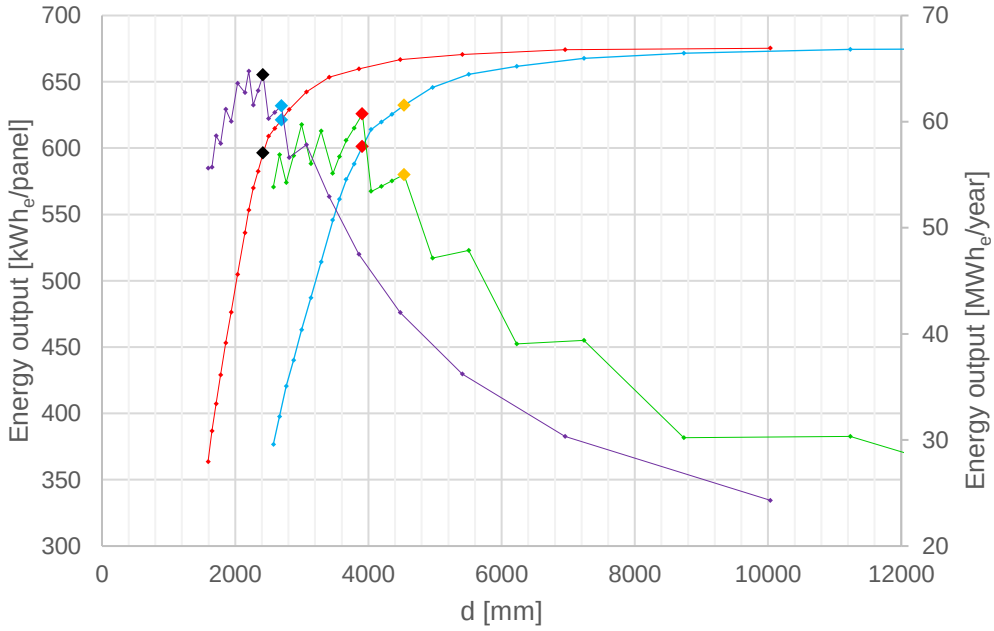

Figure 32 - Energy output (total and per panel) at surface C1 versus the distance between two rows (d).

Where the line colors correspond to the same configurations as in block B1.

In this case, there were two candidates to the optimal, which are the black and blue points (both representing horizontal configuration of the panels). The black configuration presents a considerably higher total energy output, though with a remarkably lower panel productivity. Since, as mentioned, the total output is expected to be far lower than the hospital's consumption, the total energy output was prioritized, and the black points were chosen.

These points correspond to 11 rows of 9 panels each, plus a total of 9 extra panels in the shorter rows, that is, a sum of 108 panels, exactly the same as in B1. The distance between rows (d) is again 2.42 m, implying a limit incidence angle of 22º. The maintenance aisle has a minimum width of 2.10 m (it is quite wide but installing another panel per row wound mean that this distance would be reduced to 0.41 m, which was considered too small).

For block D, an analogous calculation was carried out, leading to the results shown below in Figure 33.

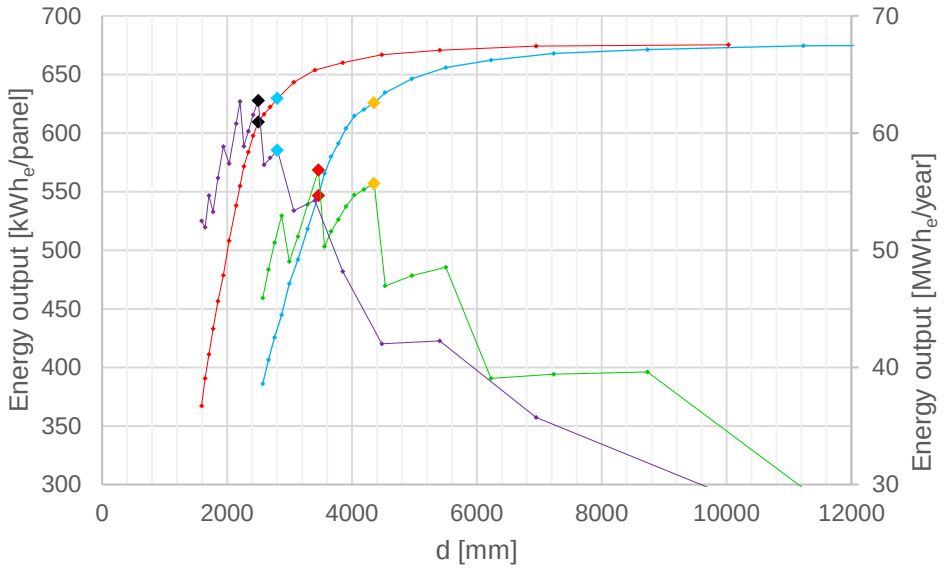

Figure 33 - Energy output (total and per panel) at surface D1 versus the distance between two rows (d).

In this case, there is no possible discussion, since the black points are clearly the best option amongst those considered, with a slightly lower total productivity but a far higher energy output per panel.

This solution implies 8 full rows of 10 horizontal panels each, with an extra number of 23 panels located in a total of 6 shorter rows, three on the Northern corner and three on the Southern. This accounts for a total of 103 panels, a slightly lower number than on B1 and C1. The distance between rows d is around 2.50 m, which corresponds to an angle α of 21º, slightly lower than on B1 and C1. The maintenance aisle will have a minimum width of 1.95 m.

The output energy per year, both total and per panel, for the aforementioned three blocks, is the following one:

Table 4 - Energy output (total and per panel) of surfaces B1, C1 and D1.

Block	*Energy output [MWhe]*	*Energy output [kWhe / panel]*
B1	64.4	596
C1	64.4	596
D1	62.8	609

From all the above, the energy output and the energy output per panel of these three areas has been calculated. Then, results obtained are extrapolated to obtain the global energy output of the other areas. Thus, the following table has been obtained:

Table 5 - Area, number of PV panels and energy output (total and per panel) of all selected surfaces.

	Area [m2]	*# panels*	*Energy [MWhe]*	*Energy [kWhe/pan]*
A1	1,364.0	277	166.4	600.6
A2	613.7	125	74.9	598.9
A3	422.7	86	51.6	599.5
A4	745.7	151	91	602.4
B1	523.6	108	64.4	596.3
B2	176.7	36	21.6	598.7
C1	523.6	108	64.4	596.3
C2	176.7	36	21.6	598.7
D1	523.6	103	62.8	609.7
D2	176.7	36	21.6	598.7
E1	446.3	91	54.4	598.2
E2	176.7	36	21.6	598.7
F	N/A	N/A	N/A	N/A
TOTAL	**5,870**	**1,193**	**716.3**	**600.4**

Finally, these calculations estimate that 1193 PV solar panels of the selected model could be installed, which would produce about 716.3 MWh of electrical energy per year. This quantity represents a 1.75% of the current electricity demand of the hospital.

5.3. Solar thermal modules

For the alternative based on solar thermal energy, the panel Baxi Sol 250H was chosen. Some considerations have been taken into account regarding the previous calculations: the panels will be oriented horizontally, fixed, facing south and tilted 38º from the horizontal plane. The rows of panels will be separated so that the limit incidence angle is 22º. The temperature at which water arrives to the tanks (which is not constant throughout the year) has been obtained from [76].

The energy output, both total and per panel, has been calculated for block B1 and extrapolated to the other areas according to their area. In block B1, 84 panels (that is, 12 rows of 7 panels each) can be installed. The distance d between two rows of panels will be 2.70 m, and the aisle width will be 1.69 m.

With this distribution, the output energy in block B1 would be 244.2 MWh_{th} per year, whilst the output energy per panel would be 2907.5 kWh_{th} per panel. When this numbers are extrapolated to the rest of the blocks, the results obtained are the ones shown in Table 6:

Table 6 - Area, number of thermal panels and energy output (total and per panel) of all selected surfaces.

	Area [m^2]	*# panels*	*Energy [MWh_{th}]*	*Energy [kWh_{th}/pan]*
A1	1364	219	636.2	2,905.1
A2	613.7	98	286.3	2,921.0
A3	422.7	68	197.2	2,899.5
A4	745.7	120	347.8	2,898.5
B1	523.6	84	244.2	2,907.5
B2	176.7	28	82.4	2,943.6
C1	523.6	84	244.2	2,907.5
C2	176.7	28	82.4	2,943.6
D1	523.6	84	244.2	2,907.5
D2	176.7	28	82.4	2,943.6
E1	446.3	72	208.2	2,891.3
E2	176.7	28	82.4	2,943.6
F	N/A	N/A	N/A	N/A
TOTAL	**5,870**	**941**	**2,738.0**	**2,909.7**

Finally, these calculations estimate that 941 PV solar panels of the selected model could be installed, which would produce about 2,738.0 MWh_{th} of thermal energy per year. This quantity represents a 244% of the current thermal energy demand of the hospital. This fact implies that, even in the case that this technology proved to be cheaper than the other technologies studied, a better solution would be to install it in only a part of the available surfaces and cover the rest with photovoltaic panels.

5.4. Hybrid photovoltaic/thermal modules

Regarding hybrid PV/T panels, the calculation procedure was the same as the one followed with thermal panels. The only difference is that two amounts needed to be taken into account, the electrical and the thermal energy, since the panels produce both of them. The chosen panel for these calculations was Abora aH72.

In block B1, and considering the same premises taken into account for thermal panels, obtaining as a result that 14 rows of 8 panels each could be installed, with a distance between rows d of 2.30 m. This accounts for a total of 112 panels in this block, with a maintenance aisle width of 1.24 m.

The energy production in this block would be 58.7 MWh_e ad 187.0 MWh_{th}, with panel productivity of 523.7 kWh_e and 1,669.6 kWh_{th} per panel. When these numbers are extrapolated to the rest of the available surface, the results are the ones shown in Table 7.

The results show that a total of 1,256 panels could be installed, producing an amount of 657.5 MWh_e and 2,096.4 MWh_{th} per year. Their productivity is around 523.5 kWh_e and 1,669.1 kWh_{th} per panel. These numbers imply a coverage of around a 1.6% of the electrical needs of the hospital, as well as a 187% of its thermal consumption.

Table 7 - Area, number of PV/T panels and energy output (total and per panel) of all selected surfaces.

	Area [m^2]	*# panels*	*Energy [MWh_e]*	*Energy [MWh_{th}]*	*Energy [kWh_e/pan]*	*Energy [kWh_{th}/pan]*
A1	1,364.0	292	152.8	487.1	523.3	1,668.3
A2	613.7	131	68.7	219.2	524.8	1,673.1
A3	422.7	90	47.3	151.0	526.1	1,677.4
A4	745.7	160	83.5	266.3	522.1	1,664.5
B1	523.6	112	58.7	187.0	523.7	1,669.6
B2	176.7	38	19.8	63.1	520.9	1,660.7
C1	523.6	112	58.7	187.0	523.7	1,669.6
C2	176.7	38	19.8	63.1	520.9	1,660.7
D1	523.6	112	58.7	187.0	523.7	1,669.6
D2	176.7	38	19.8	63.1	520.9	1,660.7
E1	446.3	95	50.0	159.4	526.2	1,677.8
E2	176.7	38	19.8	63.1	520.9	1,660.7
F	N/A	N/A	N/A	N/A	N/A	N/A
TOTAL	**5,870**	**1,256**	**657.5**	**2,096.4**	**523.5**	**1,669.1**

6. Economic analysis

Once the output energy and productivity of the different options of installation have been calculated, the cost of these options need to be estimated, since it is also a parameter of paramount importance when it comes to decide which will be the selected installation option.

6.1. Photovoltaic panels

The chosen photovoltaic panel for this installation option is the SunPower Maxeon 3. The price for this panel has been estimated to be the same as the price of other panels with the same technical specifications, which is 158.98 € including a 5% VAT [77]. The cost of the 1,193 panels would therefore be 189,663.14 €.

According to Ramos et al. [52] the cost of the panels accounts for a 58% of the total cost of a photovoltaic installation. Another 34% is attributed to the installation of those panels, whilst the remaining 8% of the total cost is related to the electrical components and fixing of the installation.

Consequently, the cost of the installation of all 1,193 panels would be 111,181.84 €, whilst the electrical components and fixing would cost 26,160.43 €. The total cost of the photovoltaic system would then be 327,005.41 €.

The cost of the electricity produced with this installation is 0.0183 €/kWh_e, which is far lower than the electricity price of the grid (of around 0.05343 €/kWh_e for a hospital [78]). Since the installation is able to produce 716.3 MWh_e per year, the savings will be around 38,271.91 €.

Considering that the panels have a lifespan of around 25 years (though it may be even longer), the evolution of the economy (considering a 3% interest rate) would be the one shown in Figure 34. The initial investment would be recovered slightly before 10 years, and the net benefit would be 359,422.04 €, as Figure 34 shows.

Throughout the 25 years of lifetime of the panels, this installation would provide a total of 17,907.5 MWh_e. At the Spanish electric grid's emission rate (around 0.19 tonnes of CO_2-eq per MWh_e generated [2]) this production would imply an emissions reduction of around 3,433 tonnes of CO_2-eq in 25 years.

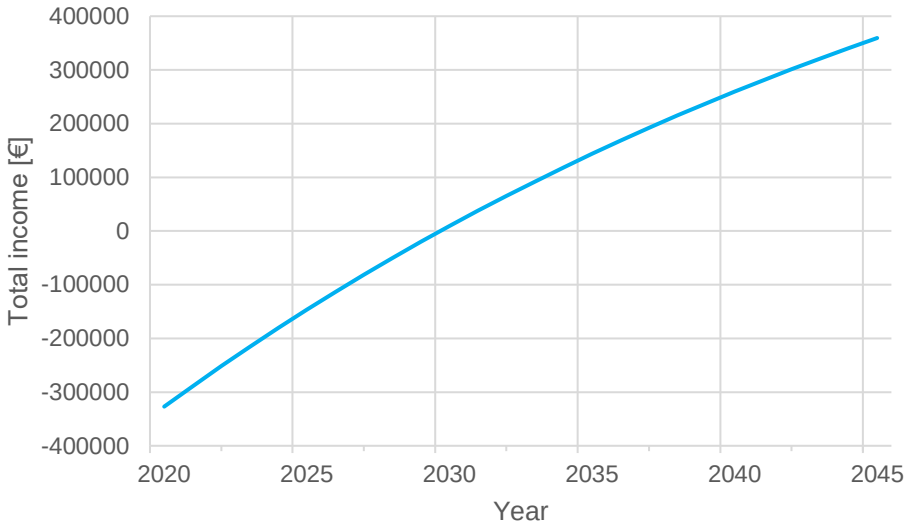

Figure 34 - Economic evolution for the installation of photovoltaic panels.

6.2. Thermal panels

The thermal panel that was selected for this option is Baxi Sol 250H, with a cost of 635.01 €, including the VAT [79]. The cost of the 941 panels of the installation in the hospital would then be 597,544.41 €.

According to Walker [80], the cost of an installed, complete water heating solar system is approximately the double of the price of the panels, so the total cost of the system may be estimated at around 1,195,088.82 €.

Altogether, the cost of the thermal energy generated by this installation would be around 0.0624 €/kWh$_{th}$. This price is higher than the price of natural gas in Spain (13.5 €/MWh in 2019) [81]. Considering this cost, the annual savings regarding the previous natural gas purchase would be around 15,148.07 €. Apart from the energy that covers the hospital's gas consumption, the panels produce another 1,615.92 MWh of thermal energy.

The energy consumption in a hospital the size of Sant Pau and in the Mediterranean area can be estimated at around 25 MWh of electrical energy and 11 MWh of thermal energy, per bed and year [72]. The ratio between the electrical and thermal energy demand is far lower than the ratio between electricity and gas consumption in Hospital de Sant Pau, which are, respectively, 40.9 GWh and 1.1 GWh, for the whole hospital per year. From this data, it is safe to assume that a part of the heating demand in the hospital is generated by electric heaters, and that this part is far larger than the 1,615.92 MWh$_{th}$ that the solar thermal panels would supply.

Given the fact that the efficiency of electric heaters can be considered to have a 100% efficiency [82], 1,615.92 MWh_e will also be saved. At the cost considered by OMIE [78], this is equivalent to an annual saving of 86,338.55 €. The savings from both gas and electricity are then 101,486.62 € per year.

A more profitable alternative, given the price difference between gas and electricity, would be to use the energy provided by the thermal panels to substitute only electric heating systems, and not those fed with gas. This way, the annual savings of the solar thermal installation would increase to 146,291.22 €.

Considering that the panels have a lifespan of around 25 years, the evolution of the economy (considering a 3% interest rate) would be the one shown in Figure 35. The initial investment would be recovered in around 10 years, and the net benefits at the end of the panels' life would be 1,428,723.52 €, as Figure 35 shows.

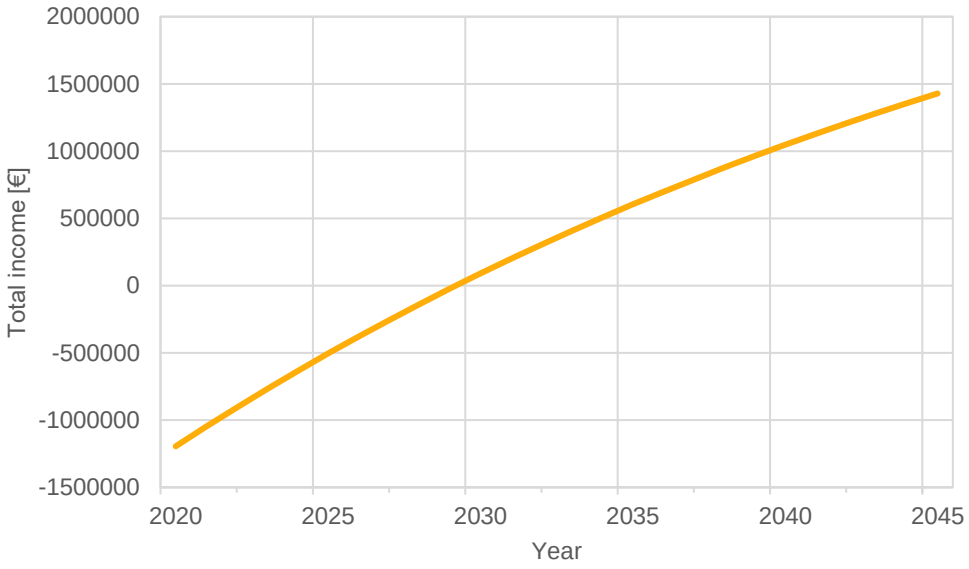

Figure 35 - Economic evolution for the installation of thermal panels.

It is interesting to compare this evolution with the one obtained if the thermal energy provided by the panels substituted all the gas consumption of the hospital instead of the electrical boilers.

Since natural gas is much cheaper than electricity, the revenue will decrease and the payback time will increase. Natural gas boilers, though, generate a higher amount of CO_2-equivalent than electric boilers (considering the emissions of electricity as the average emissions in Spanish grid electricity generation, that is, 0.19 kg CO_2-eq/kWh_e [2]). The emissions of CO_2 of natural gas boilers have been estimated at around 0.22 kg CO_2-eq/kWh [83], slightly higher than in the case of electricity.

The CO_2-eq emissions prevented by this system would be 13,123 metric tonnes throughout the panels' 25-year lifetime, in the case where the energy provided by the panels only substitutes electric-fueled thermal equipment of the hospital. If the panels' energy generation replaced the hospital's gas consumption, and with the remains a part of the electric boilers, the system would avoid the emission of 13,917 t CO_2-eq throughout 25 years.

However, this increase in CO_2-eq emission savings would come at great cost, since the revenue after 25 years would be reduced from 1,428,723.52 € to 625,128.73 € due to the natural gas' low price. Moreover, the payback time would increase significantly, from 9.20 to 14.21 years.

Overall, it seems that this extra CO_2 savings (around a 6% more) are not worth such an expenditure. If the main purpose of the installation was to maximize the emissions reduction, this difference of roughly 800,000 € could be far more useful if invested in other applications, such as purchasing newer, more efficient equipment for the hospital, or the better isolation of walls and roofs.

6.3. Hybrid PVT panels

If the implemented technology is hybrid photovoltaic-thermal panels, the chosen panel is Abora aH72, which costs 568 € per panel according to the manufacturer [84]. The cost of the 1,256 installed panels will therefore be 713,408 €.

Guarracino [85] establishes a breakdown of the capital costs of a PVT installation. Keeping the proportionality between these costs, the obtained costs of the installation will be the ones shown in *Table 8*:

Table 8 - Breakdown of the costs of the solar hybrid installation option.

Part	Cost
Collectors	713,408.00 €
Installation	212,003.32 €
Controls	50,476.98 €
Plumbing & Fixings	68,985.21 €
Tank	178,352.00 €
Pump	33,651.32 €
Total	**1,256,876.83 €**

At the current cost of electricity in Spain, specified by OMIE [78], the savings derived from the production of the 657.5 MWh_e that the installation provides are 35,132.05 €. Regarding the thermal energy provided, the same assumptions as in the thermal panels will be taken: the

generated energy will substitute the thermal demand of the hospital that is supplied via electric heaters, in order to maximize the revenue. This way, the 2,096.4 MWh_{th} generated by the thermal panels would imply savings of 112,012.34 €. The total annual savings of the installation would then be 147,144.39 €.

The cost of the generated energy by these panels would be around 0.0765 €/kWh_e if considering only the electrical output, around 0.0240 €/kWh_{th} and if considering only the thermal output. The price per kWh of energy produced, combining electrical and thermal, is around 0.0183 €/kWh.

During the following 25 years (the estimated lifespan of the panels), and considering a 3% interest rate, the economic evolution is the one shown in Figure 36. The initial investment is returned after less than 10 years, and at the end of panels' lifespan, the net revenue is 1,382,237.57 €, as Figure 36 shows.

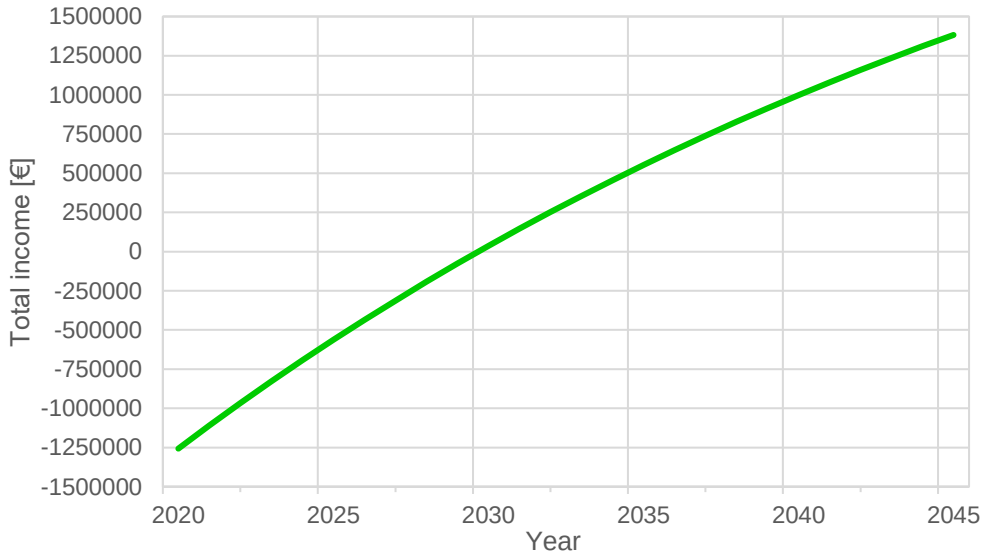

Figure 36 - Economic evolution for the installation of hybrid panels.

In an analogue way as in the case of the thermal panels, the option where the energy generated by the panels substitutes that supplied by the gas-fueled equipment instead of the electrical equipment will be analyzed.

Out of the total of 2,096.4 MWh_{th} of thermal energy generated annually by these panels, 1,122.08 MWh_{th} would replace the current gas consumption, and the remaining 974.32 MWh_{th} would substitute energy that is supplied by electrical equipment at the time being.

This way, the emissions avoided throughout the 25 years of lifetime of the panels would amount to a total of 13,993 tonnes of CO_2-eq. This quantity is not much higher (only around a

6%) than the 13,199 tonnes of CO_2-eq that would be saved if the energy supplied by the panels substituted that provided by electrical equipment.

Due to the lower price of natural gas, the yearly economic savings would be reduced, which would have a direct impact on the final revenue and the payback time. The revenue after the panels' 25-year lifetime would decrease from 1,382,237.57 € to 578,642.60 €, whilst the payback time would increase from 9.68 to 14.98 years. At first sight, it is too high a cost for such a small improvement in emissions reduction.

In a similar way than in the case of the solar thermal panels, if the emissions reduction was to be maximized at all costs, the roughly 800,000 € of difference could be put to a better use, and achieve a higher emissions reduction, if spent in other applications. One example of these applications would be the purchase of newer, more efficient equipment for the hospital, or a better isolation of walls and roofs.

6.4. Comparison

Once the three installation options have been defined and analyzed, they may be compared in order to determine which one will be chosen. Table 9 shows the main characteristics that need to be taken into account for this comparison.

Table 9 - Comparison between the different technology options.

	Photovoltaic	Thermal	PVT
Production [MWh/y]	716	2,738	2,754
CO_2-eq saved [t]	3,433	13,123	13,199
Cost [€/kWh]	0.0183	0.0175	0.0183
Investment [€]	327,005	1,195,089	1,256,877
Revenue$_{25\ years}$ [€]	359,422	1,428,724	1,382,238
Payback time [y]	9.68	9.20	9.68

The comparison shows similar results for the three alternatives in terms of cost per unit of energy produced, and in the three cases the economic revenue after 25 years is slightly higher than the initial investment. The payback time is also similar in the three alternatives, being between 9 and 10 years. In all these categories, though, the thermal alternative seems to be marginally better than the other ones.

These results are subject to the considered prices of all the components involved in the installation. Since the three alternatives are similar, any variations in these prices could easily make one of them stand out either way.

In terms of energy production and CO_2-eq emissions avoided, which are proportional characteristics, the photovoltaic option produces far less energy, only around a 26% of the energy generated via the other technologies, though in terms of the required investment this proportion is maintained.

It seems, then, that all three options are perfectly viable and that any of them would be a useful option in order to reduce both the greenhouse gases emissions and the energy dependency of the hospital. Each of the options is slightly better in one characteristic or another: the photovoltaic alternative requires a far lower investment; the thermal is more cost-effective and provides a higher revenue (both in absolute numbers and per euro invested) and the hybrid option maximizes energy production and CO_2-eq emissions savings.

Another issue to take into account is the fact that, when purchasing such a large number of panels (1193 for a photovoltaic installation, 941 for thermal or 1256 for hybrid) their price will most likely decrease significantly compared with the considered price, which is the catalogue price for a single panel. Hence, the cost of the installation for all three cases would be lower and the payback time shorter.

The data found regarding this price reduction is related to the photovoltaic-thermal panels, and suggests a discount of at least 30% in the panels' price for the required 1,256 panels [84]. This price reduction was not considered for the calculations since it was only found for the hybrid panels and not for the other options.

All in all, and though none of the three alternatives outstands amongst the others, the chosen option is the solar thermal installation, due to its high energy production and greenhouse gases emissions savings. The ratio between the final revenue and the initial investment, as well as the final revenue, is the highest among the three options.

7. Environmental analysis

After the selected system has been established and its characteristics and cost defined, its impact on the environment must be studied.

7.1. Emissions

The generation of electrical energy that is not produced by renewable sources, as well as the burning of hydrocarbons, imply the emission of an amount of greenhouse gases. In the case of Hospital de Sant Pau, the energy-related emissions are originated in the production of the consumed electrical energy and in the burning of natural gas in boilers located in the hospital.

The emissions generated by the production of the electrical energy consumed in the hospital, considering a demand of 40,890,758 kWh per year and an emission factor of 0.19 kg CO_2-eq per kWh generated [2], are around 7,769.24 tonnes of CO_2-eq per year.

Regarding the emissions produced by burning natural gas, considering the demand of 1,122,079 kWh and an emission factor of around 0.22 kg CO_2-eq per kWh produced [83], the emissions are 246.86 tonnes of CO_2-eq per year. The global amount of energy-related emissions generated by the hospital are then around 8,016.1 tonnes of CO_2-eq per year.

Since the selected installation provides clean, renewable energy which substitutes energy generated via conventional technologies, it will cause a reduction in the greenhouse gases emissions of the hospital.

The energy generated by the solar thermal installation is 2,737,997.78 kWh per year, implying a yearly reduction of 520.22 tonnes of CO_2-eq emissions. This amount represents around a 6.49% of the current emissions of the hospital.

7.2. Life Cycle Assessment

The analyzed system is the solar power installation which was defined in chapter 5, including not only the panels but also the rest of the components that form the installation. This analysis will include all the processes involved, including the extraction and production of materials, manufacturing, assembly, installation, maintenance cycles and all the intermediate transportations including the end-of-life transportation to the landfill.

The solar thermal installation described previously consists of the following components: the aforementioned 941 solar thermal collectors Baxi Sol 250H, their fastening system to the roof and the water tanks, pumps and valves that are required by the system.

A schematic view of the components and processes that the manufacturing of these components imply, as well as the materials used, is shown in Figure 37.

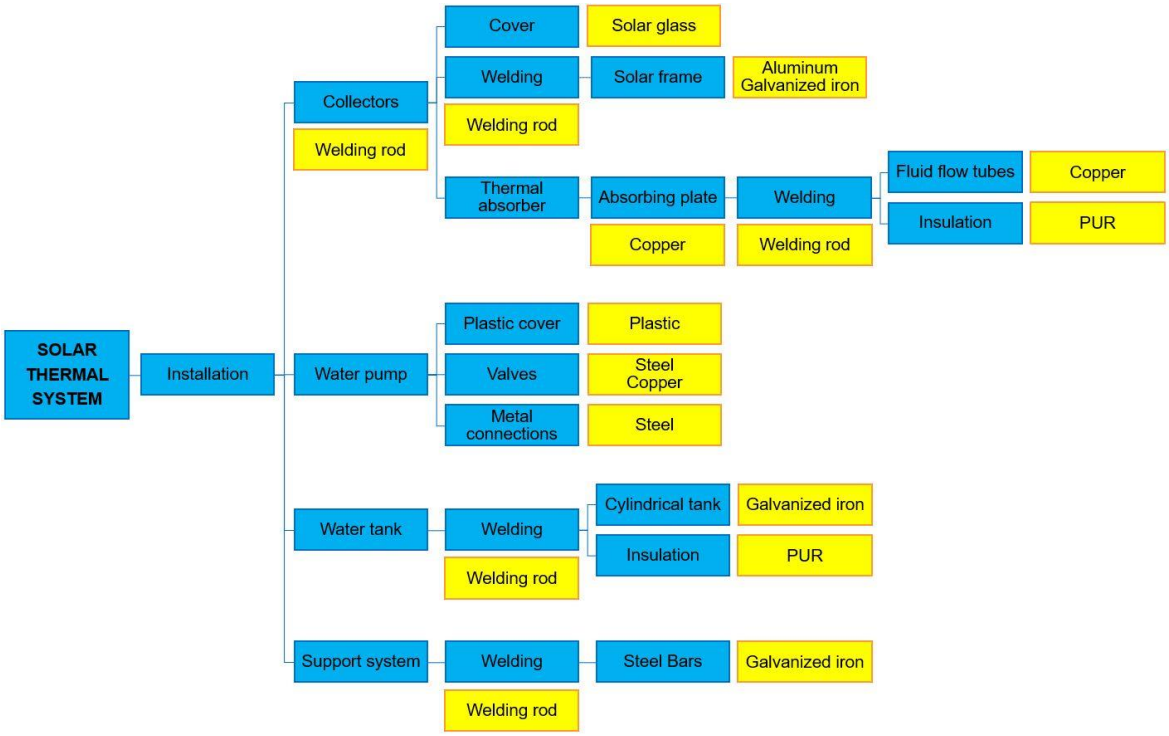

Figure 37 - Flow chart of the fabrication and installation process of the thermal solar system (adapted from [86]*).*

The energy obtained from the solar panels in Ardente et al. [87] are around 6.2 GJ per year, that is, around 1.72 MWh. The weather in Palermo is similar to Barcelona's, so it was considered to be the same, and the solar panels' characteristics were also considered to be the same. Extrapolating from this amount of energy to the energy production in the installation, the mass input of the materials used for the installation during the entire life cycle assessment could be estimated, obtaining the results shown in Table 10.

Table 10 - Mass input of the materials used for the installation (adapted from [87]*).*

Material	Input mass [tonnes]
Galvanized steel	179.01
Thermal fluid	59.62
Stainless steel	46.26
Copper	21.62
Glass	16.69
Rigid PUR	14.31
Aluminum	6.36
Cardboard	4.77
Epoxy dust	1.75
Steel	1.59
HDPE	1.43
LDPE	1.27
Magnesium	1.14
Welding rods	0.48
Brass	0.22
Flexible PUR	0.05
PVC	0.05

The emissions generated to the air during the aforementioned processes throughout the life cycle are the ones shown in Table 11.

Table 11 - Air emissions generated throughout the life cycle (adapted from [87]*).*

Pollutant	Air emissions [tonnes]
CO2	1,044.50
CO	7.15
SO2	5.72
CH4	3.50
NOx	2.86
Dust	0.95
NMVOC	0.48
Mn	0.48
Cr	0.02
Ni	0.01

These emissions, when expressed in terms of tonnes of CO_2 equivalent in order to unify them, represent an amount of 1,146.25 t CO_2-eq.

Clearly, the process of obtaining the raw materials, processing them into the panels, tanks, pumps and other components of the solar thermal system, along with the transportation of these parts, takes its toll on the environment. However, the amount of clean energy that this system will generate will imply even higher savings (of 13,123.23 t CO_2-eq). Then, the net

emissions saving will be 11,976.98 t CO_2-eq, which corresponds to a 5.98% of the current energy-derived emissions of the hospital, making the installation environmentally viable.

The emissions generated (mostly during the extraction of materials and the manufacturing and installation of the components) would be compensated by the emissions savings of the system shortly. At the annual emissions savings rate of around 524.93 t CO_2-eq, the initial emissions would be compensated after only 2.18 years.

The impact of the system could be much lower if the materials used were to be recycled at the end of the life cycle. According to the Bank of America Merryl Lynch, the production of a tonne of steel requires around 1.5 tonnes of iron ore [88], and the World Coal Association estimates that around 770 kg of coal are also needed [89]. Norstar states that, for each tonne of steel made from scrap steel, 1,115 kg of iron ore and 625 kg of coal are saved [90], which is around a 77% of the required materials.

Some other of the most used materials in the installation, such as copper, aluminum, glass or PUR are also recyclable, and almost in their totality. This means that a very high percentage of the materials used (those listed on Table 10 above) may be re-used at the end of the life cycle of the installation, reducing the energy required in the processing of these materials up to 85% in some cases such as copper [91], and further reducing its environmental impact.

Conclusions

This project's main purpose was the design of a solar-based self-consumption energy system in Hospital de Sant Pau, in Barcelona. This installation's objective is to produce renewable energy, thus decreasing the greenhouse gases emissions and reducing the energy dependency of the hospital and by extension of the city of Barcelona.

The designed installation, based on flat plate solar thermal panels, results in a reduction of the hospital's energy dependency, as it is able to produce around a 6.5% of the hospital's energy demand. The energy produced in this installation alone would represent around a 2% of the total energy generated in the city of Barcelona, according to 2017 data [14].

The installation is found to be economically viable, with a final revenue of around 1.43 million €, which is higher than the required initial investment, and with a payback time of slightly more than 9 years. The other studied alternatives (photovoltaic and hybrid installations) are also economically viable, presenting similar results.

The greenhouse gases emissions reduction achieved with this installation throughout the 25 years of lifetime of the solar panels is 13,123 tonnes of CO_2-eq. This amount of emissions savings represents around a 6.5% of the current emissions derived from the hospital's energy consumption.

To conclude, the life cycle assessment that was carried out shows that there is an important amount of emissions derived from the extraction of materials and the manufacturing, transportation, assembly and installation of components. However, these emissions are low compared to those saved by the installation, and even when taking them into account, the emissions reduction is 11,977 tonnes of CO_2-eq, or a 6% of the previous ones.

Acknowledgements

I would like to express my gratitude to Rubèn Moragues, General Services Director of Hospital de Sant Pau, for the extremely interesting guided visit around the hospital's installations and for the energy consumption data provided.

I would also like to acknowledge the assistance provided by my tutor Dr. Alba Ramos, for her invaluable advice and assistance in the development and correction of the project.

Finally, I would like to express my very great appreciation to my family for their patience, understanding and encouragement throughout the elaboration of this study.

Bibliography

[1] RED ELÉCTRICA DE ESPAÑA (REE). *El Sistema Eléctrico Español 2019*. Madrid, Red Eléctrica de España, 2020, p. 26-27, 36, 43.

[2] RED ELÉCTRICA DE ESPAÑA (REE). *Emisiones de CO_2 asociadas a la generación de electricidad en España*. Madrid, Red Eléctrica de España, 2020, p. 2-3.

[3] EUROPEAN COMMISSION. *Emissions in the automotive sector*. [https://ec.europa.eu/growth/sectors/automotive/environment-protection/emissions_en, accessed on June 26th, 2020]

[4] EUROPEAN COMMISSION. *2030 climate & energy framework*. https://ec.europa.eu/clima/policies/strategies/2030_en, accessed on June 26th, 2020]

[5] EUROPEAN COMMISSION. *2050 long-term strategy*. https://ec.europa.eu/clima/policies/strategies/2050_en, accessed on June 26th, 2020]

[6] Real Decreto 244/2019, de 5 de abril, por el que se regulan las condiciones administrativas, técnicas y económicas del autoconsumo de energía eléctrica (BOE-A-2019-5089). Ministerio para la Transición Ecológica. Madrid, April 6th, 2019.

[7] Ley 24/2013, de 26 de diciembre, del Sector Eléctrico (BOE-A-2013-13645). Jefatura del Estado. Madrid, December 27th, 2013.

[8] Código Técnico de la Edificación (CTE). (2006). *Documento Básico de Ahorro de Energía*. (DB-HE).

[9] Directive 2010/31/EU of the European Parliament and of the Council of 19 May 2010 on the energy performance of buildings.

[10] Directive 2012/27/EU of the European Parliament and of the Council of 25 October 2012 on energy efficiency.

[11] Directive (EU) 2018/2001 of the European Parliament and of the Council of 11 December 2018 on the promotion of the use of energy from renewable sources.

[12] Directive 2009/28/EC of the European Parliament and of the Council of 23 April 2009 on the promotion of the use of energy from renewable sources.

[13] EUROPEAN COMMISSION. *Energy use in buildings*. [https://ec.europa.eu/energy/eu-buildings-factsheets-topics-tree/energy-use-buildings_en, accessed on June 27th, 2020]

[14] AGÈNCIA D'ENERGIA DE BARCELONA. *Balanç d'energia i emissions de gasos amb efecte hivernacle de Barcelona 2017*. Barcelona, Ajuntament de Barcelona, 2019, p. 3, 6.

[15] WORLD HERITAGE CONVENTION OF THE UNESCO. *Palau de la Música Catalana and Hospital de Sant Pau, Barcelona*. [http://whc.unesco.org/en/list/804, accessed on March 25th, 2020]

[16] SEDE ELECTRÓNICA DEL CATASTRO. *Consulta y certificación de Bien Inmueble*. [https://www1.sedecatastro.gob.es/CYCBienInmueble/OVCConCiud.aspx?del=8&mun=900&UrbRus=U&RefC=1051501DF3815A0001HK&Apenom=&esBice=&RCBice1=&RCBice2=&DenoBice=&from=nuevoVisor&ZV=NO, accessed on March 29th, 2020]

[17] ENCYCLOPÆDIA BRITANNICA. *Mediterranean climate*. https://www.britannica.com/science/Mediterranean-climate, accessed on March 28th, 2020]

[18] PEEL, M.C. et al. (2007). Updated world map of the Köppen-Geiger climate classification. Hydrology and Earth System Sciences Discussions, European Geosciences Union, 2007, 4 (2), p. 439-473. hal-00298818.

[19] PETERSON, A. (2020). *Köppen climate types of Iberia*. Online picture, obtained from: [https://commons.wikimedia.org/wiki/File:K%C3%B6ppen_climate_types_of_Iberia.png, accessed on March 28th, 2020]

[20] KÖPPEN, W. (1900). *Versuch einer Klassifikation der Klimate, vorzugsweise nach ihren Beziehungen zur Pflanzenwelt*. Online document, obtained from [http://koeppen-geiger.vu-wien.ac.at/pdf/Koppen_1900.pdf, accessed on March 28th, 2020]

[21] METEOBLUE. *Clima Barcelona.* [https://www.meteoblue.com/es/tiempo/historyclimate/climatemodelled/barcelona_espa%c3%b1a_3128760, accessed on March 30th, 2020]

[22] GLOBAL SOLAR ATLAS. [https://globalsolaratlas.info/detail?c=41.360576,2.029724,11&s=41.413525,2.171268&m=site, accessed on March 30th, 2020]

[23] EUROPEAN COMMISSION. *Photovoltaic Geographical Information System* (PVGIS). [https://re.jrc.ec.europa.eu/pvg_tools/en/tools.html#MR, accessed on March 30th, 2020]

[24] NATIONAL RENEWABLE ENERGY LABORATORY. *Solar resource data and tools*. [https://www.nrel.gov/grid/solar-resource/renewable-resource-data.html, accessed on March 31st, 2020]

[25] MESSENGER, R. and ABTAHI, H. (2017). *Photovoltaic Systems Engineering*. Boca Raton, Taylor & Francis Group, 49-57, 398-434. ISBN 978-1-4987-7277-8.

[26] ENCYCLOPÆDIA BRITANNICA. *Photoelectric effect*. [https://www.britannica.com/science/photoelectric-effect, accessed on February 16th, 2020]

[27] GUINJOAN, F. *3. PV cells & PV generators*. Escola Tècnica Superior d'Enginyeria Industrial de Barcelona, UPC, Barcelona. October 2018.

[28] REINDERS, A. et al. (2017). *Photovoltaic solar energy: from fundamentals to applications*. Chichester, John Wiley & Sons Ltd, p. 80-81, 507. ISBN 9781118927472.

[29] PENDEM, S. R. and MIKKILI, S. (2018). *Modeling, simulation and performance analysis of solar PV array configurations (Series, Series-Parallel and Honey-Comb) to extract maximum power under Partial Shading Conditions*. Energy Reports, 4 (2018), 274-287. DOI: https://doi.org/10.1016/j.egyr.2018.03.003

[30] CLEAN ENERGY REVIEWS, *Solar Panel Construction*. [https://www.cleanenergyreviews.info/blog/solar-panel-components-construction, accessed on February 16th, 2020]

[31] AL-HABAHBEH, O. M. et al. (2014). *Durability Assessment on Monocrystalline Photovoltaic Cells*. Zaytoonah University International Engineering Conference on Design and Innovation in Sustainability 2014. Paper Code No. 1569893641.

[32] POWER FROM SUNLIGHT, *Important Facts about EVA (ethylene vinyl acetate) Film for Solar PV Panels*. [https://www.powerfromsunlight.com/important-facts-about-eva-ethylene-vinyl-acetate-film-for-solar-pv-panels/, accessed on February 18th, 2020]

[33] TARGRAY, *PV Backsheet Material Solution for Photovoltaic Manufacturing*. [https://www.targray.com/solar/pv-backsheet, accessed on February 18th, 2020]

[34] SOLAR POWER WORLD. The PV junction box: An overlooked, yet important part of a solar panel. [https://www.solarpowerworldonline.com/2017/05/pv-junction-box-overlooked-yet-important-part-solar-panel/, accessed on February 18th, 2020]

[35] FRAUNHOFER INSTITUTE FOR SOLAR ENERGY SYSTEMS, ISE. (2020). *Photovoltaics Report*. Freiburg, Fraunhofer Institute.

[36] ENERGYSAGE. *Monocrystalline and polycristalline solar panels: what you need to know*. [https://www.energysage.com/solar/101/monocrystalline-vs-polycrystalline-solar-panels/, accessed on March 1st, 2020]

[37] SOLARQUOTES. *Polycrystalline vs monocrystalline solar panels*. [https://www.solarquotes.com.au/panels/photovoltaic/monocrystalline-vs-polycrystalline/, accessed on March 1st, 2020]

[38] AURORA SOLAR BLOG. *Solar Panel Wiring Basics: An Intro to How to String Solar Panels*. [https://blog.aurorasolar.com/solar-panel-wiring-basics-an-intro-to-how-to-string-solar-panels, accessed on February 29th, 2020]

[39] ALTERNATIVE ENERGY TUTORIALS. *Solar Panel Orientation*. https://www.alternative-energy-tutorials.com/solar-power/solar-panel-orientation.html, accessed on March 18th, 2020]

[40] SOLAR FEEDS. *Types of Solar Trackers and their Advantages & Disadvantages*. [https://solarfeeds.com/solar-trackers-types-and-its-advantages-and-disadvantages/, accessed on February 28th, 2020]

[41] NOU, J. et al. (2016). *A new approach to the real-time assessment of the clear-sky direct normal irradiance*. Applied Mathematical Modelling (2016). DOI: 10.1016/j.apm.2016.03.022.

[42] ALTERNATIVE ENERGY TUTORIALS. *Solar Cell I-V Characteristic*. http://www.alternative-energy-tutorials.com/energy-articles/solar-cell-i-v-characteristic.html, accessed on February 25th, 2020]

[43] ENERGY EDUCATION. *Solar cell efficiency*. https://energyeducation.ca/encyclopedia/Solar_cell_efficiency, accessed on February 25th, 2020]

[44] MCEVOY, A. et al. (2011). *Practical Handbook of Photovoltaics. Fundamentals and Applications*. Oxford, Elsevier, p. 417-419. ISBN 9780123859341.

[45] THE RENEWABLE ENERGY HUB. *How do solar thermal panels work*. [https://www.renewableenergyhub.co.uk/main/solar-thermal-information/how-do-solar-thermal-panels-work/, accessed on March 4th, 2020]

[46] NORTON, B. (2014). *Harnessing solar heat*. Dordrecht, Springer, p. 91-111. ISBN 978-94-007-7274-8.

[47] SOLAR ENERGY. *Components of a solar thermal installation*. [https://solar-energy.technology/solar-thermal/installation, accessed on March 12th, 2020]

[48] KALOGIROU, S. A. (2004). *Solar thermal collectors and applications*. Progress in Energy and Combustion Science, 30 (2004), 231-295. DOI: https://doi.org/10.1016/j.pecs.2004.02.001

[49] SOLAR ENERGY. *Medium temperature thermal solar energy*. [https://solar-energy.technology/solar-thermal/medium-temperature, accessed on March 15th, 2020]

[50] ALTERNATIVE ENERGY TUTORIALS. *Evacuated Tube Collector*. [http://www.alternative-energy-tutorials.com/solar-hot-water/evacuated-tube-collector.html, accessed on March 13th, 2020]

[51] APRICUS. *Evacuated Tubes*. [https://www.apricus.com/Evacuated-Tubes-pd90770826.html, accessed on March 15th, 2020]

[52] RAMOS, A. et al. (2017). *Solar Thermal and Hybrid Photovoltaic-Thermal Systems for Renewable Heating*. Grantham Institute Briefing Paper No 22.

[53] BHATIA, S. C. (2014). *Advanced Renewable Energy Systems*. New Delhi, Woodhead Publishing India Pvt. Ltd., p. 97-109. ISBN 978-93-80308-43-2.

[54] TRIPLE PUNDIT. *4 Things to Consider Before Going Solar Thermal*. https://www.triplepundit.com/story/2011/4-things-consider-going-solar-thermal/80236, accessed on March 5th, 2020]

[55] JRADI, M. and RIFFAT, S. (2012). *Medium temperature concentrators for solar thermal applications*. International Journal of Low-Carbon Technologies 9, 214-224. DOI: 10.1093/ijlct/cts068.

[56] BREEZE, P. (2016). *Solar Power Generation*. London, Elsevier, p. 17-46. ISBN 978-0-12-804004-1.

[57] GS ENERGY. *Parabolic Trough*. [https://www.gsenergy.eu/parabolic-trough/, accessed on March 18th, 2020]

[58] INTERNATIONAL RENEWABLE ENERGY AGENCY. (2012). *Concentrating Solar Power*. Abu Dhabi, IRENA, p. 4-10.

[59] MIRANDA, A. Graph showing parts of a hybrid solar panel with water heater, Renewable Energy, Vector Image. [https://www.shutterstock.com/es/image-vector/graph-showing-parts-hybrid-solar-panel-1469337449, accessed on March 27th, 2020]

[60] MELLOR, A. et al. (2018). *Roadmap for the next generation of hybrid photovoltaic-thermal solar energy collectors*. Solar Energy, 174 (2018), 386-398. DOI: https://doi.org/10.1016/j.solener.2018.09.004.

[61] CHOW, T. T. (2009). *A review on photovoltaic/thermal hybrid solar technology*. Applied Energy 87, 365-379. DOI: 10.1016/j.apenergy.2009.06.037.

[62] GS ENERGY. *Photovoltaic Thermal Hybrid Solar Collector*. [https://www.gsenergy.eu/photovoltaic-thermal-hybrid-solar-collector/, accessed on March 13th, 2020]

[63] Kaundinya, D. P. et al. (2009). *Grid-connected versus stand-alone energy systems for decentralized power – A review of literature*. Renewable and Sustainable Energy Reviews 13 (2009), 2041–2050.

[64] THE ELECTROPÆDIA. *Lead Acid Batteries*. [https://www.mpoweruk.com/leadacid.htm, accessed on May 24th, 2020]

[65] EUROBAT. (2016). *Battery energy storage in the EU. Barriers, opportunities, services and benefits*. Eurobat. Obtained from https://www.eurobat.org/images/news/publications/eurobat_batteryenergystorage_web.pdf.

[66] ELECTRONICS NOTES. *Lithium Ion Battery Advantages & Disadvantages*. [https://www.electronics-notes.com/articles/electronic_components/battery-technology/li-ion-lithium-ion-advantages-disadvantages.php, accessed on May 26th, 2020]

[67] BLOOMBERG NEF. *A Behind the Scenes Take on Lithium-ion Battery Prices*. [https://about.bnef.com/blog/behind-scenes-take-lithium-ion-battery-prices/, accessed on March 19th, 2020]

[68] DO IT YOURSELF. *NiCd Battery: Advantages and Disadvantages*. [https://www.doityourself.com/stry/nicd-battery-advantages-and-disadvantages, accessed on May 28th, 2020]

[69] INTERNATIONAL RENEWABLE ENERGY AGENCY. (2013). *Thermal Energy Storage. Technology Brief*. IRENA, p. 3-13.

[70] DODARO, J. *Molten Salt Storage*. Coursework for PH240, Stanford University, Fall 2015. [http://large.stanford.edu/courses/2015/ph240/dodaro2/, accessed on August 29th, 2020]

[71] Pedrajas, J. (2017). *Auditoría energética de un hospital* (Master Thesis). Escuela Técnica Superior de Ingeniería (ICAI), Universidad Pontificia Comillas, Madrid.

[72] Mínguez, C. (2018). *Consumos de Energía en Hospitales Españoles*. IDAE. Ingeniería Hoy.

[73] HOSPITAL DE LA SANTA CREU I SANT PAU. *Plànol de l'hospital*. [http://www.santpau.cat/documents/125011/687716/planol+1/983d4d9a-ca6a-49e3-a194-eecae4afce59, accessed on April 7th, 2020]

[74] VECTORSTOCK. [https://cdn2.vectorstock.com/i/1000x1000/36/66/blue-wind-rose-vector-20943666.jpg, accessed on April 7th, 2020]

[75] IKASKUNTZA BIRTUAL ETA DIGITALIZATUEN LHII. *2.2.1. – Cálculo de la separación de las filas de paneles para evitar sombras*. [https://ikastaroak.ulhi.net/edu/es/IEA/ISF/ISF05/es_IEA_ISF05_Contenidos/website_221_clculo_de_la_separacin_de_las_filas_de_paneles_para_evitar_sombras.html, accessed on April 4th, 2020]

[76] ENERGÍAS RENOVABLES EN ESPAÑA SUELO SOLAR. *Temperatura del agua de red en capitales de provincia de España (ºC).* [https://suelosolar.com/guia/acs-solar/temperatura-agua-ciudades, accessed on April 7th, 2020]

[77] AUTOSOLAR. *Placa Solar 400W Jinko Mono Perc*. [https://autosolar.es/panel-solar-24-voltios/placa-solar-400w-jinko-mono-perc, accessed on May 2nd, 2020]

[78] Operador del Mercado Ibérico de Energía (OMIE). (2019). *Evolución del Mercado de electricidad. Informe anual 2019*.

[79] GASFRÍOCALOR. *Captador solar plano Baxi SOL 250 H*. [https://www.gasfriocalor.com/captador-solar-plano-baxi-sol-250-h, accessed on July 15th, 2020]

[80] WALKER, A. (2013). *Solar energy*. Hoboken, John Wiley & Sons, Inc, p. 165-168. ISBN 978-1-118-13924-0.

[81] Comisión Nacional de los Mercados y la Competencia (CNMC). *Informe de supervisión del mercado de gas natural en España. Período: año 2019*. Madrid, CNMC, 2020.

[82] DEPARTMENT OF ENERGY. *Electric Resistance Heating*. [https://www.energy.gov/energysaver/home-heating-systems/electric-resistance-heating, accessed on July 28th, 2020]

[83] PARLIAMENTARY OFFICE OF SCIENCE AND TECHNOLOGY OF THE UK PARLIAMENT (POST). (2016). *Carbon Footprint of Heat Generation*. London, Parliamentary Office of Science and Technology, Note 523, May 2016.

[84] ABORA ENERGY. (2020). *Tarifas 2020. Panel aH72 SK. Precios instalador partner.* Abora Energy, S.L., 2020.

[85] Guarracino, I. et al. (2016). *Performance assessment and comparison of solar ORC and hybrid PVT systems for the combined distributed generation of domestic heat and power*. Imperial College London. [https://www.researchgate.net/publication/305882623, accessed on July 20th, 2020]

[86] Souliotis, M. et al. (2018). *Experimental study and Life Cycle Assessment (LCA) of Hybrid Photovoltaic/Thermal (PV/T) solar systems for domestic applications*, Renewable Energy, doi: 10.1016/j.renene.2018.04.01.

[87] Ardente, F. et al. (2004). *Life cycle assessment of a solar thermal collector: sensitivity analysis, energy and environmental balances*. Renewable Energy 30, 109-130. doi:10.1016/j.renene.2004.05.006

[88] BUSINESS INSIDER AUSTRALIA. *This is how iron ore is turned into steel*. [https://www.businessinsider.com.au/how-is-steel-made-blast-furnace-2017-11, accessed on August 24th, 2020]

[89] WORLD COAL ASSOCIATION. *How is steel produced?* [https://www.worldcoal.org/coal/uses-coal/how-steel-produced, accessed on August 25th, 2020]

[90] NORSTAR STEEL RECYCLERS. *Recycling benefits.* [https://www.norstar.com.au/benefits/, accessed on August 25th, 2020]

[91] COPPER ALLIANCE. *Europe's demand for copper is increasingly met by recycling*. [https://copperalliance.eu/benefits-of-copper/recycling/, accessed on August 26th, 2020]